

## Supplementary Information: Altering the solubility of metal-organic polyhedra via pendant functionalization of $\text{Cp}_3\text{Zr}_3\text{O}(\text{OH})_3$ nodes

Meghan G. Sullivan,<sup>a</sup> Gregory E. Sokolow,<sup>a</sup> Eric T. Jensen,<sup>b</sup> Matthew R. Crawley,<sup>a</sup> Samantha N. MacMillan,<sup>c</sup> Timothy R. Cook\*<sup>a</sup>

a. Department of Chemistry, University at Buffalo, The State University of New York, Buffalo, New York 14260, United States.

b. Chemistry Instrument Center, Department of Chemistry, University at Buffalo, State University of New York, Buffalo, NY 14260, United States.

c. Department of Chemistry and Chemical Biology, Cornell University, Ithaca, New York 14853, United States.

### Table of Contents

Characterization .....	2
Instrumental methods.....	2
NMR spectroscopy .....	3
Mass spectrometry.....	19
Infrared spectroscopy .....	24
X-Ray Crystallography .....	25
Instrumental methods.....	25
ZrMOP-ben .....	26
ZrMOP-vb .....	28
ZrMOP-tfmb .....	30
Solubility Studies .....	34
Instrumental methods.....	34
Materials .....	34
Solution preparation & digestion .....	34
Instrument Calibration .....	34
Results .....	36
References .....	37

## Characterization

### *Instrumental methods*

<sup>1</sup>H Nuclear magnetic resonance (NMR) spectra were acquired using a Bruker AVANCE NEO 500 spectrometer. Chemical shifts ( $\delta$ ) are reported in parts per million (ppm) referenced using the residual protio solvent peaks as internal standards. Multiplicities are indicated as singlets (s), doublets (d), triplets (t) or multiplets (m).

High-Resolution Mass spectrometry (HRMS) experiments for **ZrMOP** and **ZrMOP-ben** were completed using a 12 T Bruker Solarix FT-ICR-MS. Samples were prepared in methanol and directly injected with a syringe into the instrument at 2  $\mu$ L/min and ionized via electrospray ionization (ESI) at 5.5 kV. ESI, ion transfer optics, quadrupole, and analyzer parameters were tuned prior to analysis and remained constant throughout the experiments. The collision cell parameters were optimized for each sample. The collision voltage (entrance) for **ZrMOP** was -2.0 V with a DC extract bias (entrance) of 1.2 V. The collision voltage (entrance) for **ZrMOP-ben** was -5.0 V with a DC extract bias (entrance) of 1.2 V. The spectra reported are from 20 scans and 40 scans for **ZrMOP** and **ZrMOP-ben**, respectively.

A Thermo Fisher Q-Exactive Liquid Chromatograph Orbitrap Tandem Mass Spectrometer was used for ESI-HRMS of **ZrMOP-vb** and **ZrMOP-tfmb**. Samples dissolved in methanol were infused at a rate of 5  $\mu$ L/min. The heated electrospray ionization (HESI) source in positive ionization mode used a sheath gas flow rate of 20 psi, aux gas flow rate of 5, spray voltage of 5.5 kV, capillary temperature of 300°C, and S-lens RF level set to 80. Data was collected using a scan range from m/z 500-3000, and a resolution of 70,000. 100 scans were acquired for both samples.

For data acquired on the Q-Exactive, isotope patterns were simulated at the instrument set resolution of 70,000 for each ionic formula using the simulation tool available through QualBrowser in the Xcalibur software (Thermo Scientific, San Jose, CA, USA). For data acquired using the Bruker Solarix FT-ICR-MS the isotopic patterns were simulated using the Simulate Isotopic Pattern tool for the respective ionic formulas in the Bruker Compass DataAnalysis Software (Bruker Daltonics, Bremen, Germany).

For each MOP, the predominant spectral features are the 2+, 3+, and 4+ charge states of the intact polyhedra. The respective charges are due to loss of chloride counter ions and/or proton(s). The base peak for each MOP is the 3+ charge state ( $[M]-4Cl^-H^+$ ). The proposed elemental formulas were confirmed with appropriate isotopic patterns when compared to the simulated patterns, and error was calculated in ppm.

Fourier transform infrared (FTIR) spectra were acquired with a PerkinElmer 1760 FTIR spectrometer with horizontal attenuated total reflectance (ATR) on neat ZrMOP powders.

NMR spectroscopy

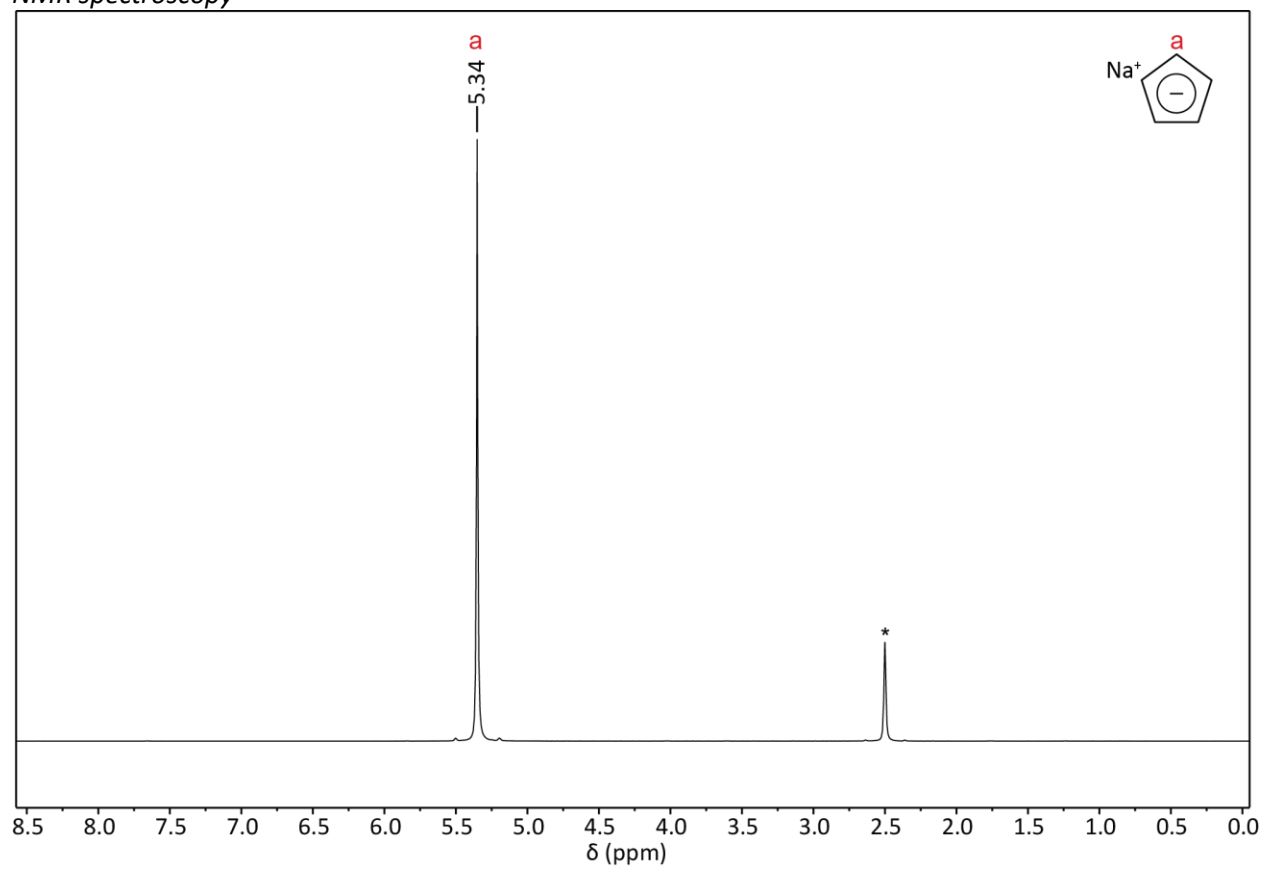


**Figure S1.**  $^1\text{H}$  NMR spectrum of NaCp (500 MHz,  $\text{DMSO-d}_6$ ,  $25^\circ\text{C}$ ). Asterisk (\*) corresponds to DMSO (2.50 ppm).

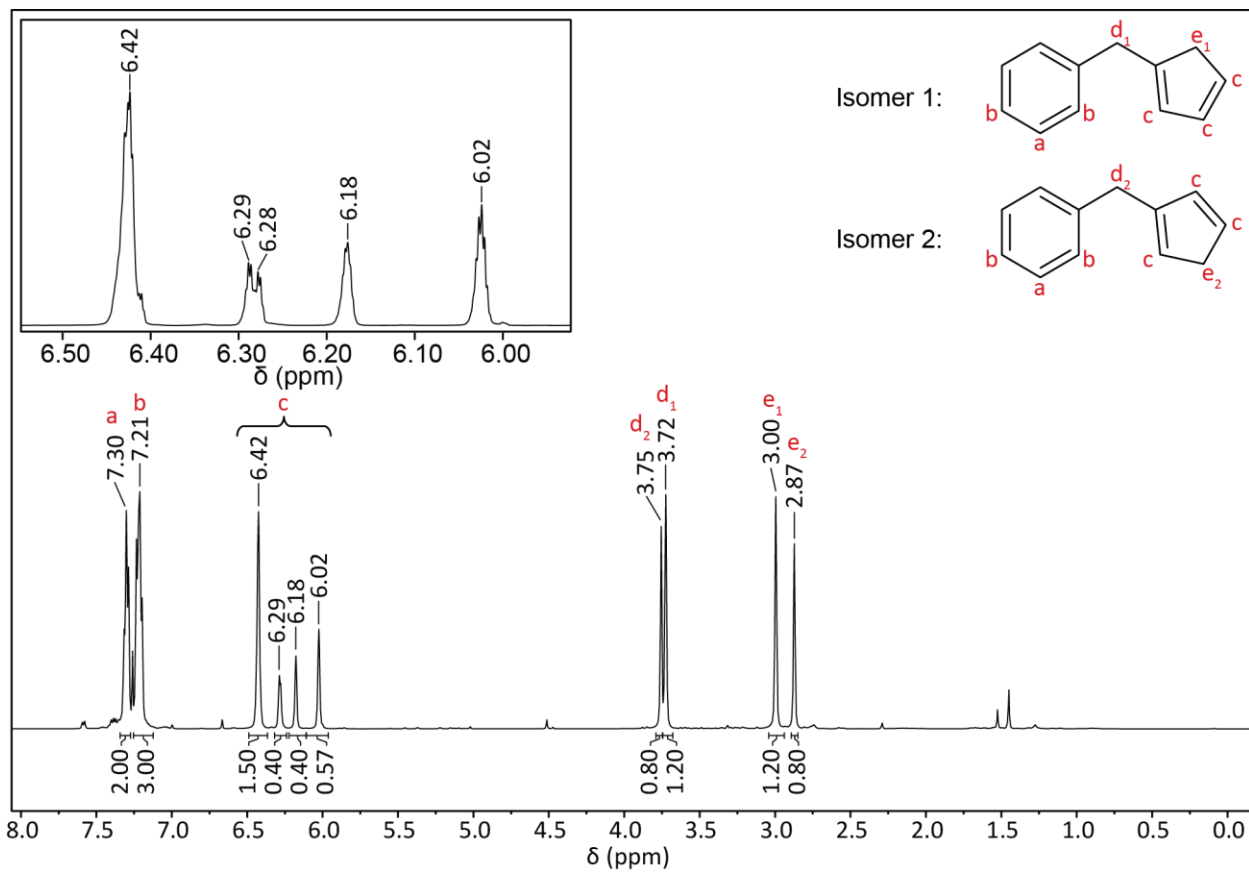


**Figure S2.** <sup>1</sup>H NMR spectrum of (benzyl)cyclopentadiene (500 MHz, CDCl<sub>3</sub>, 25°C). CHCl<sub>3</sub> (7.26 ppm) is directly in-between peaks a and b.

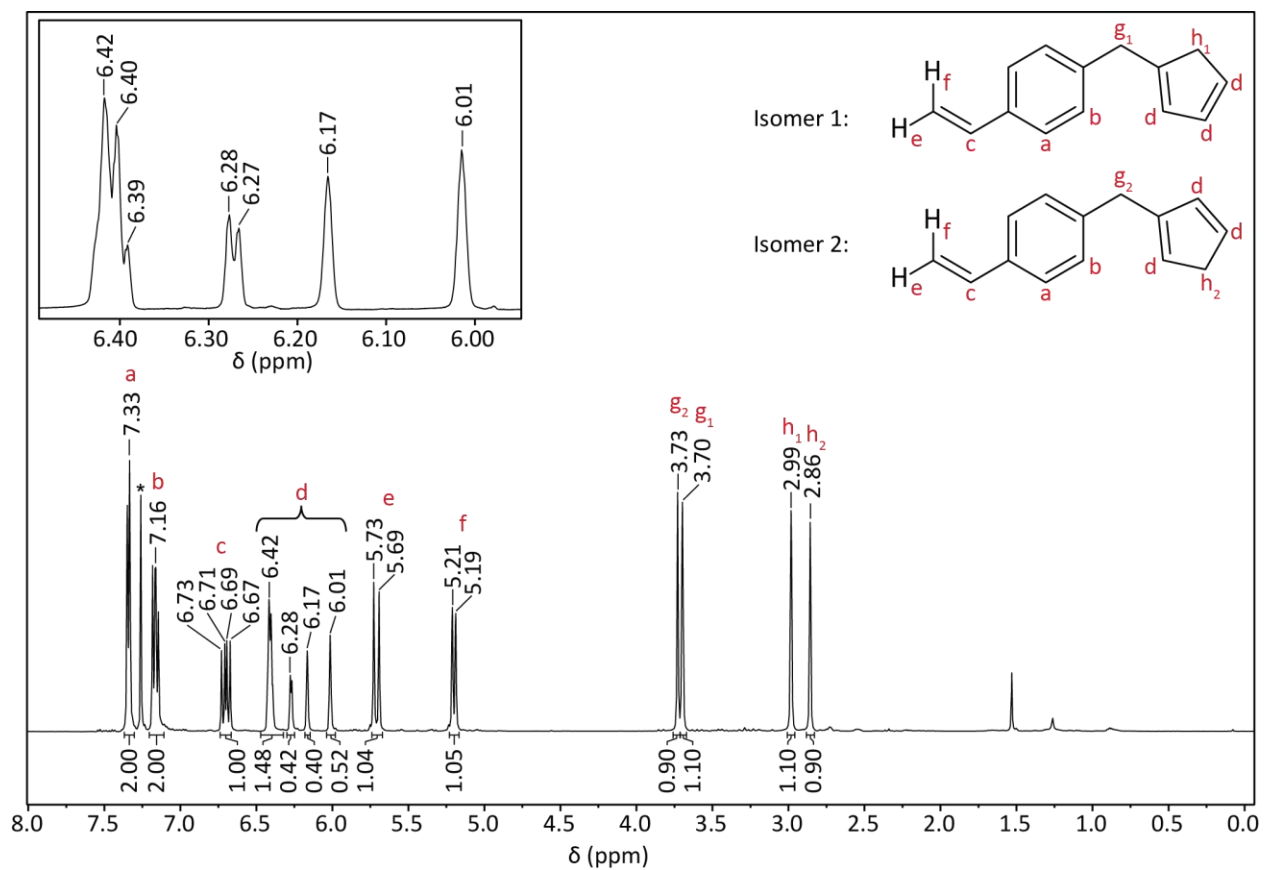


**Figure S3.**  $^1\text{H}$  NMR spectrum of  $(p\text{-vinylbenzyl})\text{cyclopentadiene}$  (500 MHz,  $\text{CDCl}_3$ ,  $25^\circ\text{C}$ ). Asterisk (\*) corresponds to  $\text{CDCl}_3$  (7.26 ppm).

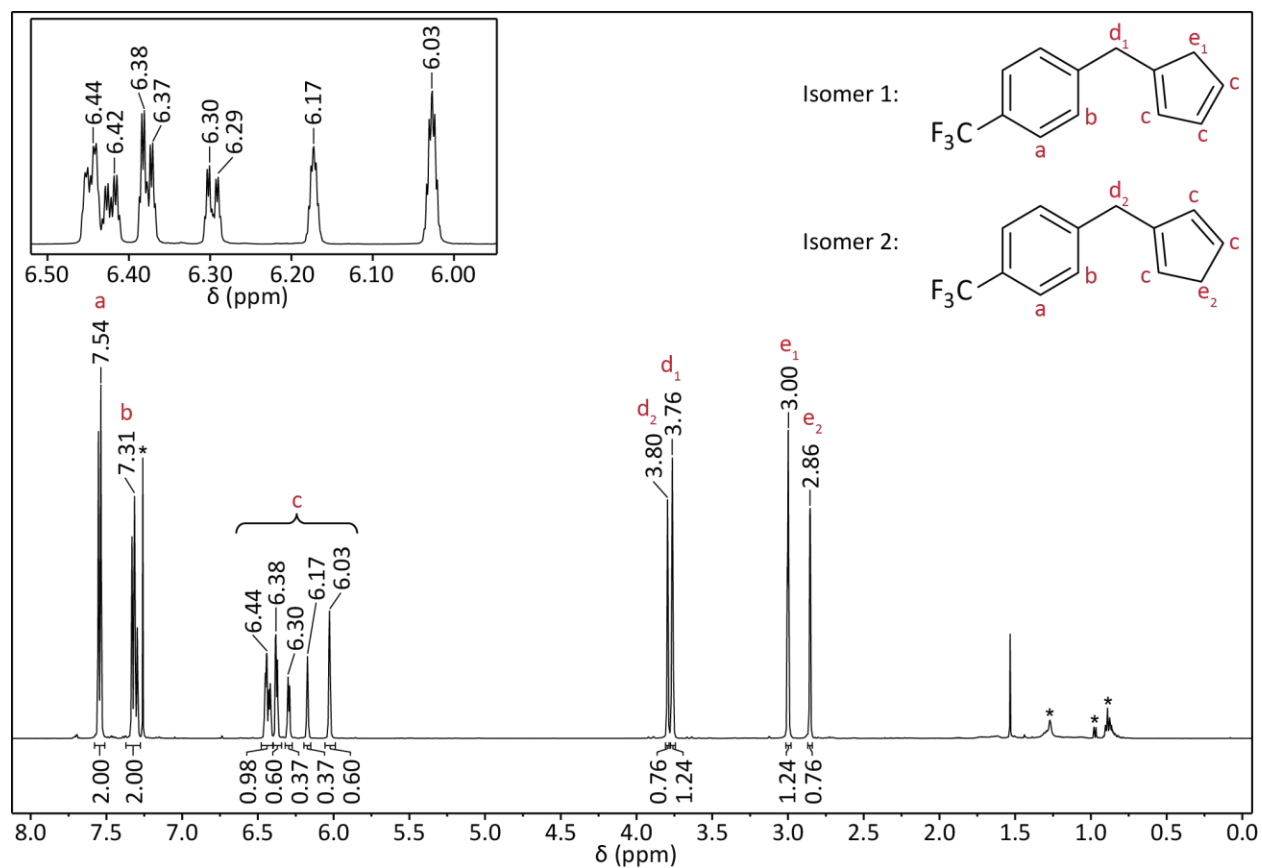


**Figure S4.**  $^1\text{H}$  NMR spectrum of  $(p\text{-trifluoromethylbenzyl})\text{cyclopentadiene}$  (500 MHz,  $\text{CDCl}_3$ ,  $25^\circ\text{C}$ ). Asterisks (\*) correspond to  $\text{CHCl}_3$  (7.26 ppm), and residual hexanes (0.89, 0.98, 1.27 ppm).

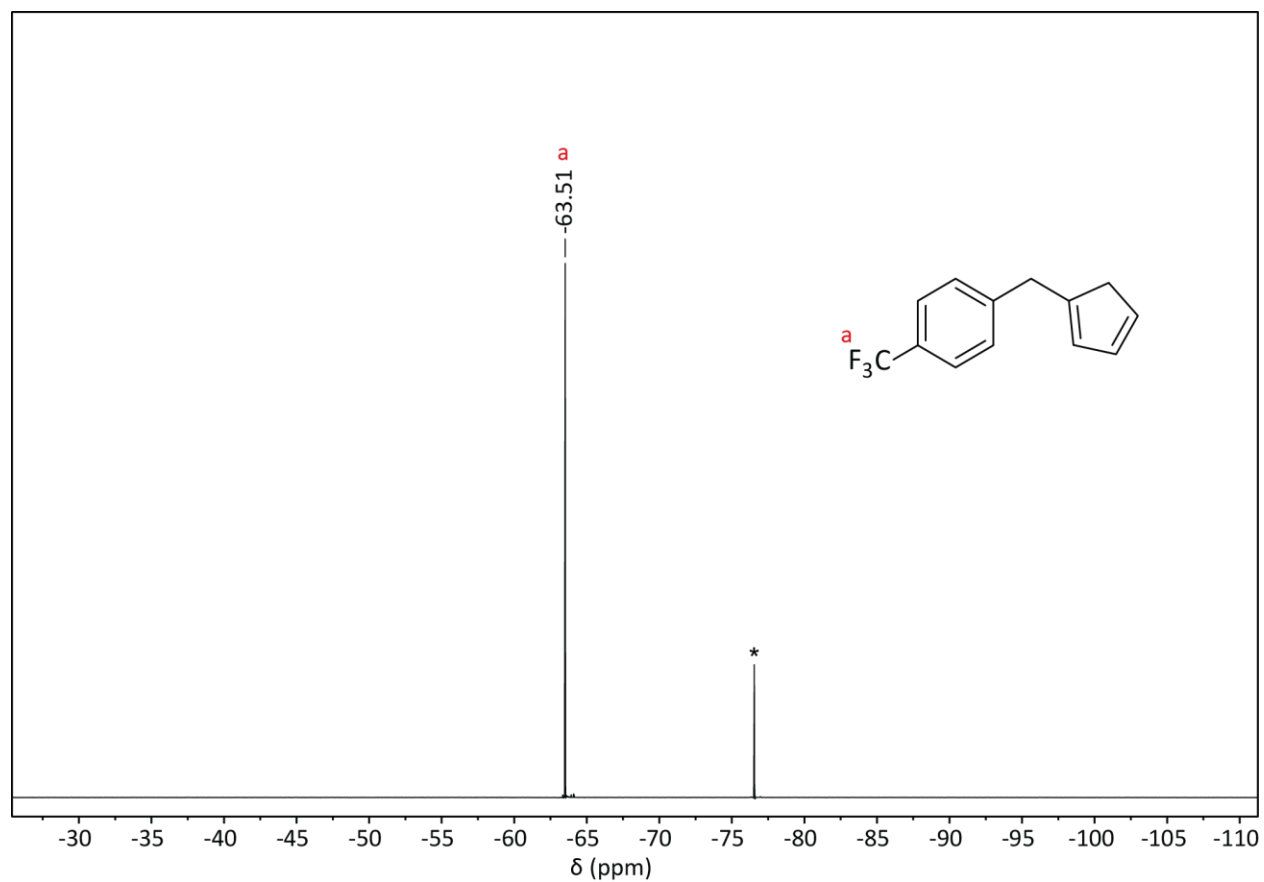


**Figure S5.**  $^{19}\text{F}$  NMR spectrum of (*p*-trifluoromethylbenzyl)cyclopentadiene (470 MHz,  $\text{CDCl}_3$ ,  $25^\circ\text{C}$ ). Asterisk (\*) corresponds to trifluoroacetic acid reference ( $-76.55$  ppm).

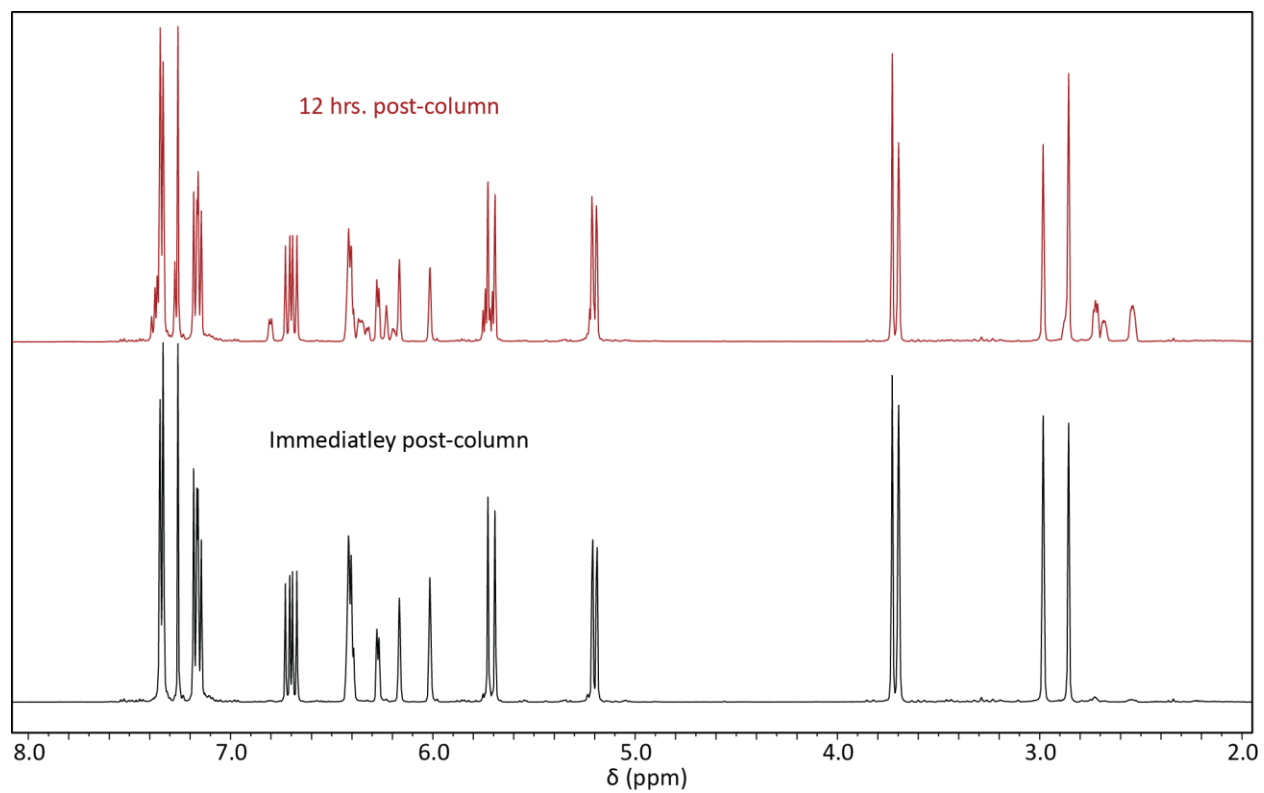


**Figure S6.** <sup>1</sup>H NMR spectrum of (*p*-vinylbenzyl)cyclopentadiene (500 MHz, CDCl<sub>3</sub>, 25°C) immediately after purification by column chromatography (bottom), and 12 hours later (top) showing evidence of degradation.

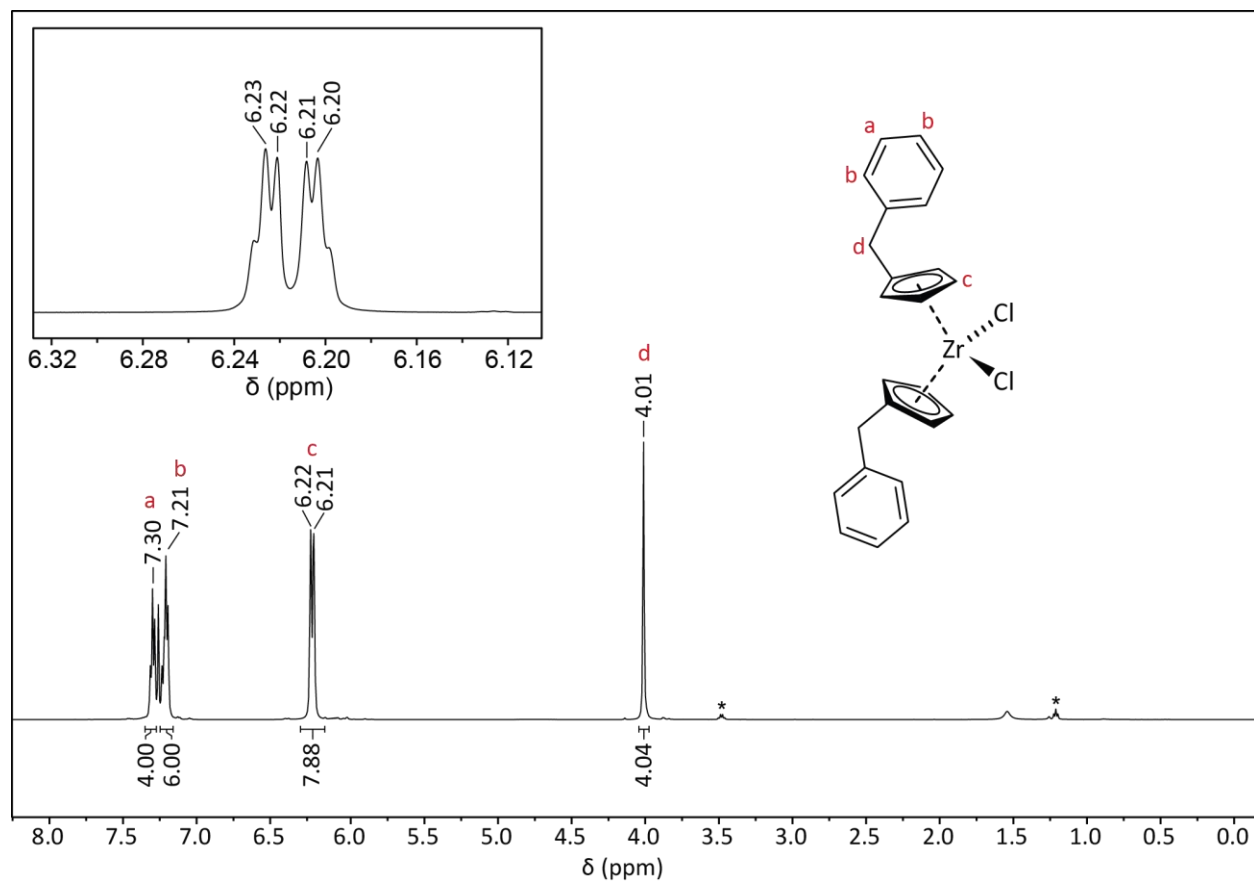


**Figure S7.**  $^1\text{H}$  NMR spectrum of (benzylcyclopentadiene)zirconium dichloride (500 MHz,  $\text{CDCl}_3$ ,  $25^\circ\text{C}$ ). Asterisks (\*) correspond to residual diethyl ether (3.48, 1.21 ppm).  $\text{CHCl}_3$  (7.26 ppm) is directly in-between peaks a and b.

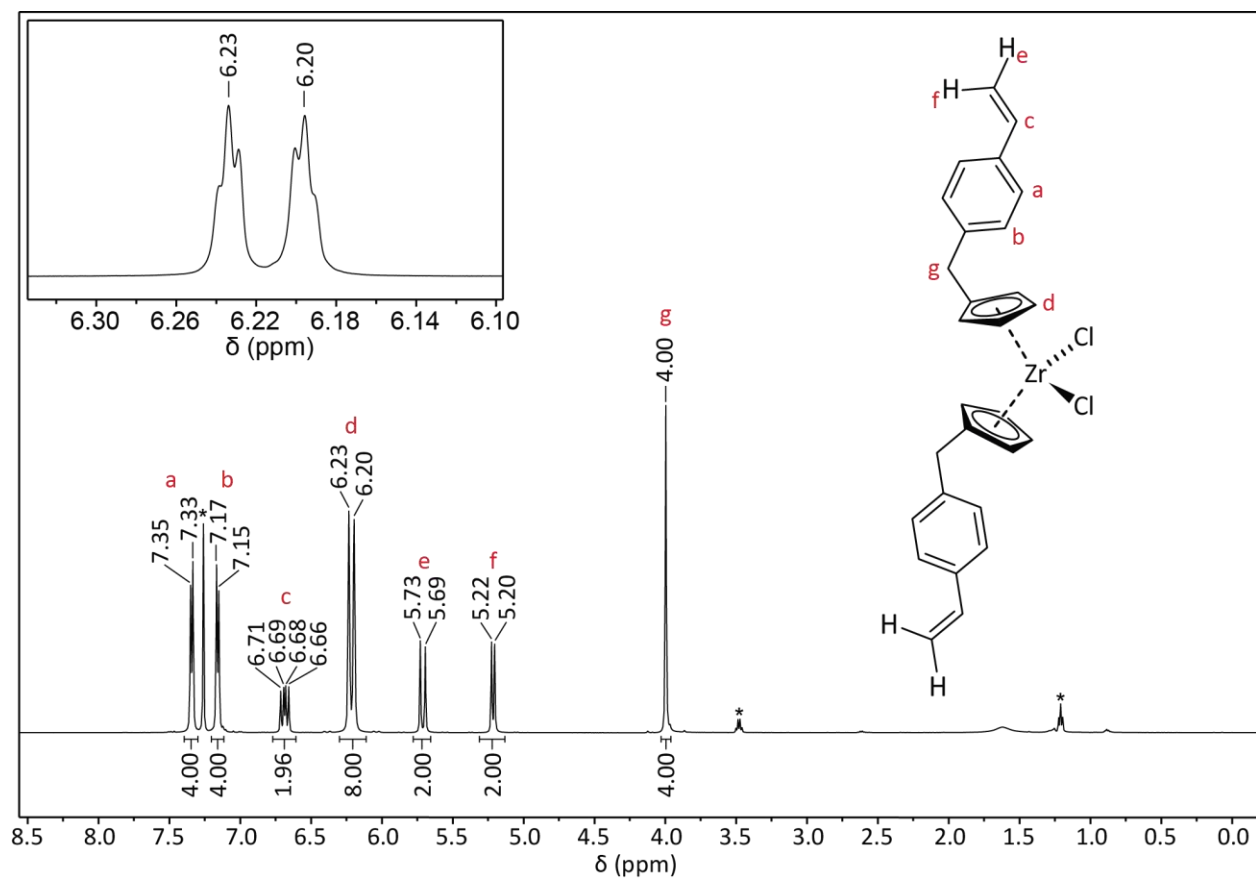


**Figure S8.**  $^1\text{H}$  NMR spectrum of  $(p\text{-vinylbenzylcyclopentadiene})\text{zirconium dichloride}$  (500 MHz,  $\text{CDCl}_3$ ,  $25^\circ\text{C}$ ). Asterisks (\*) correspond to  $\text{CHCl}_3$  (7.26 ppm), and residual diethyl ether (3.48, 1.21 ppm).

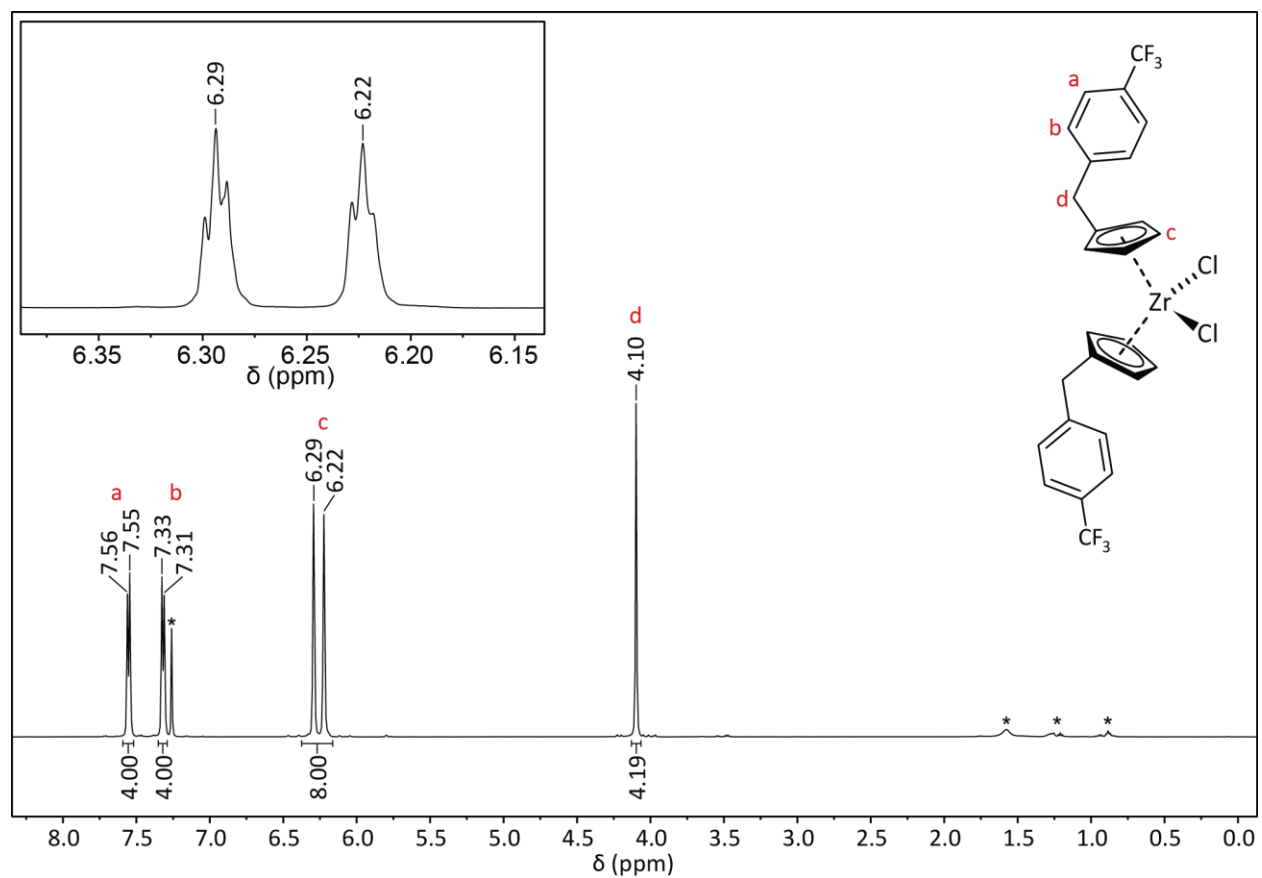


**Figure S9.**  $^1\text{H}$  NMR spectrum of  $(p\text{-trifluoromethylbenzylcyclopentadiene})\text{zirconium dichloride}$  (500 MHz,  $\text{CDCl}_3$ ,  $25^\circ\text{C}$ ). Asterisks (\*) correspond to  $\text{CHCl}_3$  (7.26 ppm) and residual hexanes (0.75 – 1.75 ppm).

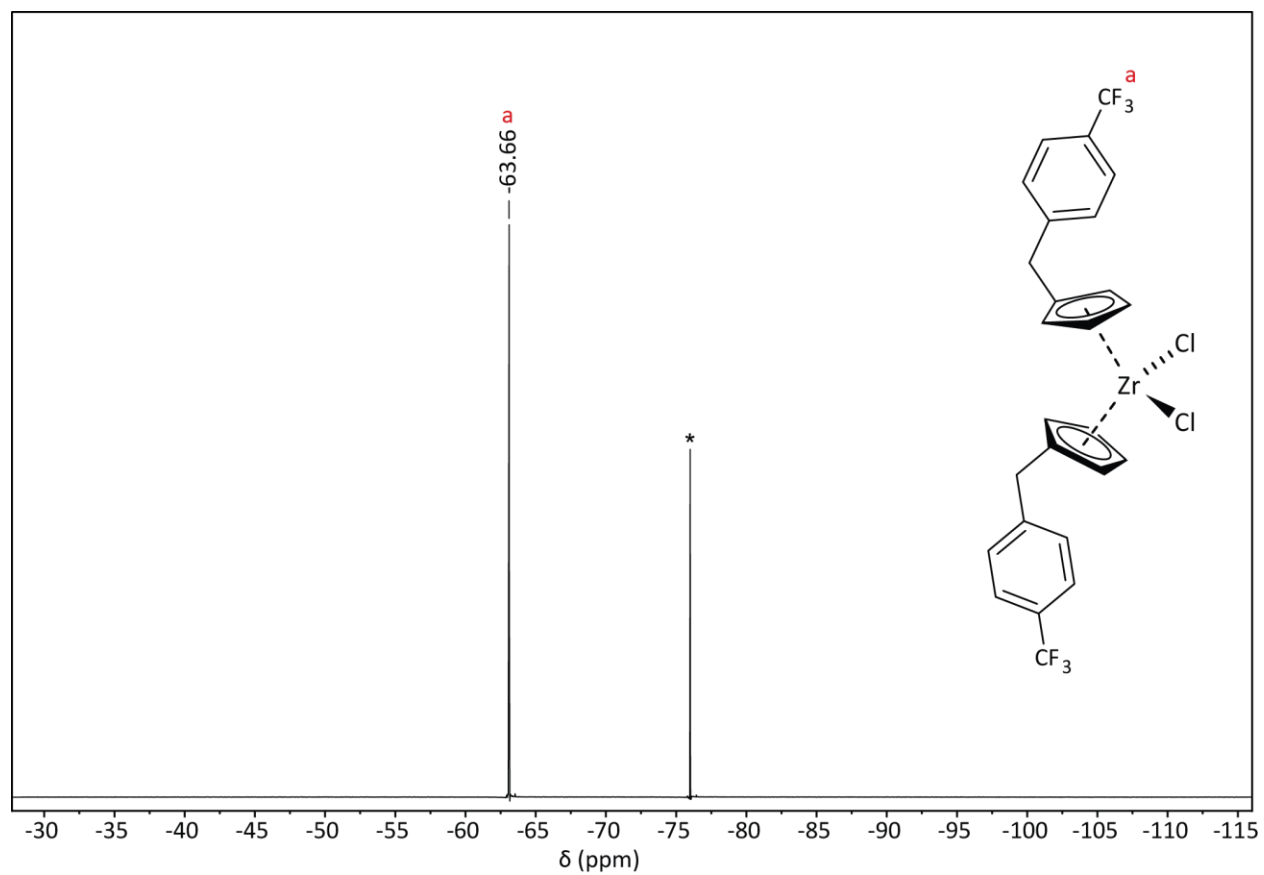


**Figure S10.**  $^{19}\text{F}$  NMR spectrum of  $(p\text{-trifluoromethylbenzylcyclopentadiene})\text{zirconium dichloride}$  (470 MHz,  $\text{CDCl}_3$ ,  $25^\circ\text{C}$ ). Asterisk corresponds to trifluoroacetic acid reference ( $-76.55$  ppm).

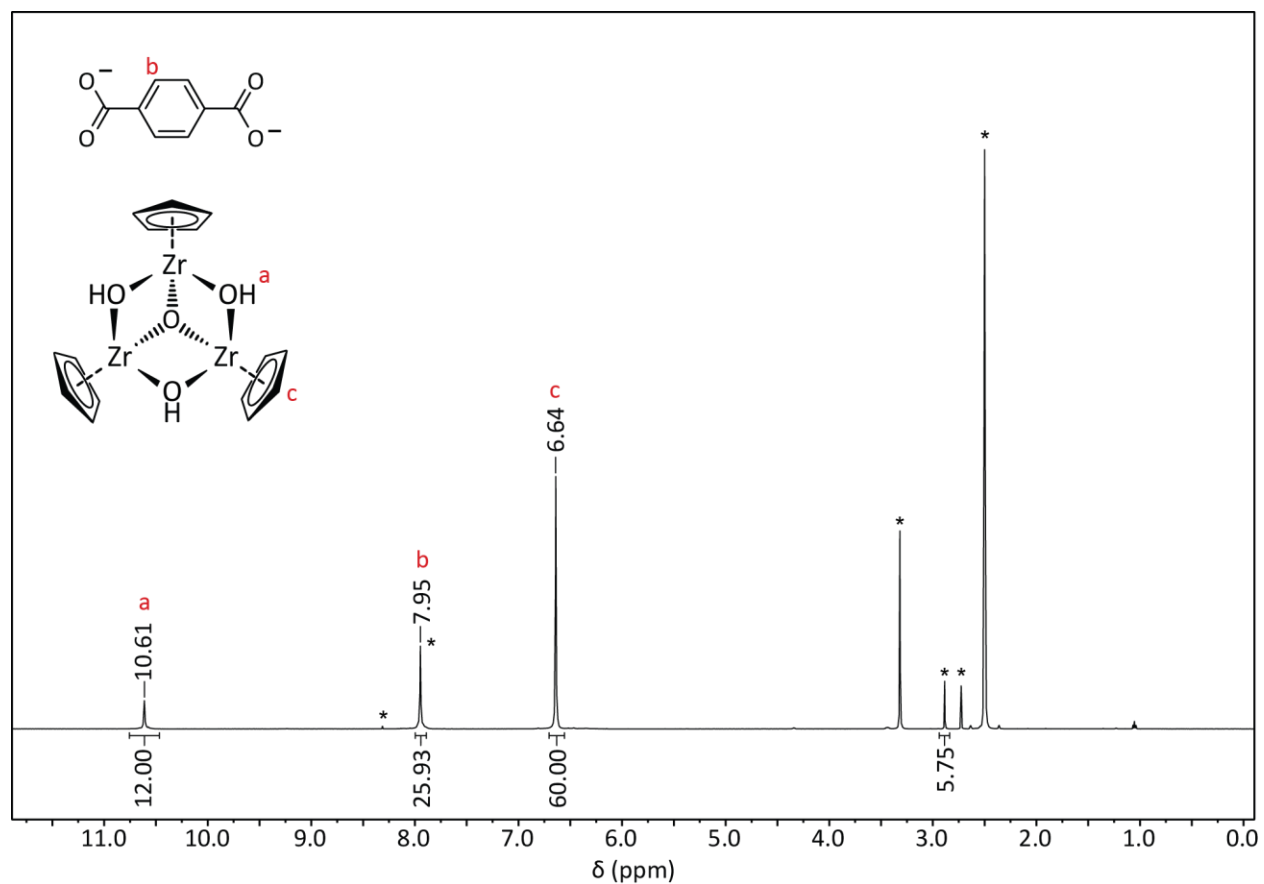


**Figure S11.**  $^1\text{H}$  NMR spectrum of **ZrMOP-bdc** (500 MHz,  $\text{DMSO-d}_6$ ,  $25^\circ\text{C}$ ). Asterisks (\*) correspond to  $\text{CHCl}_3$  (8.31 ppm), DMF (7.95, 2.89, 2.73 ppm),  $\text{H}_2\text{O}$  (3.34 ppm), and DMSO (2.50 ppm).  $\text{CH}_3$  of DMF is integrated to show the contribution from the DMF CH ( $\sim 1.9\text{H}$ ) under the 1,4-bdc CH signal at 7.95 ppm.

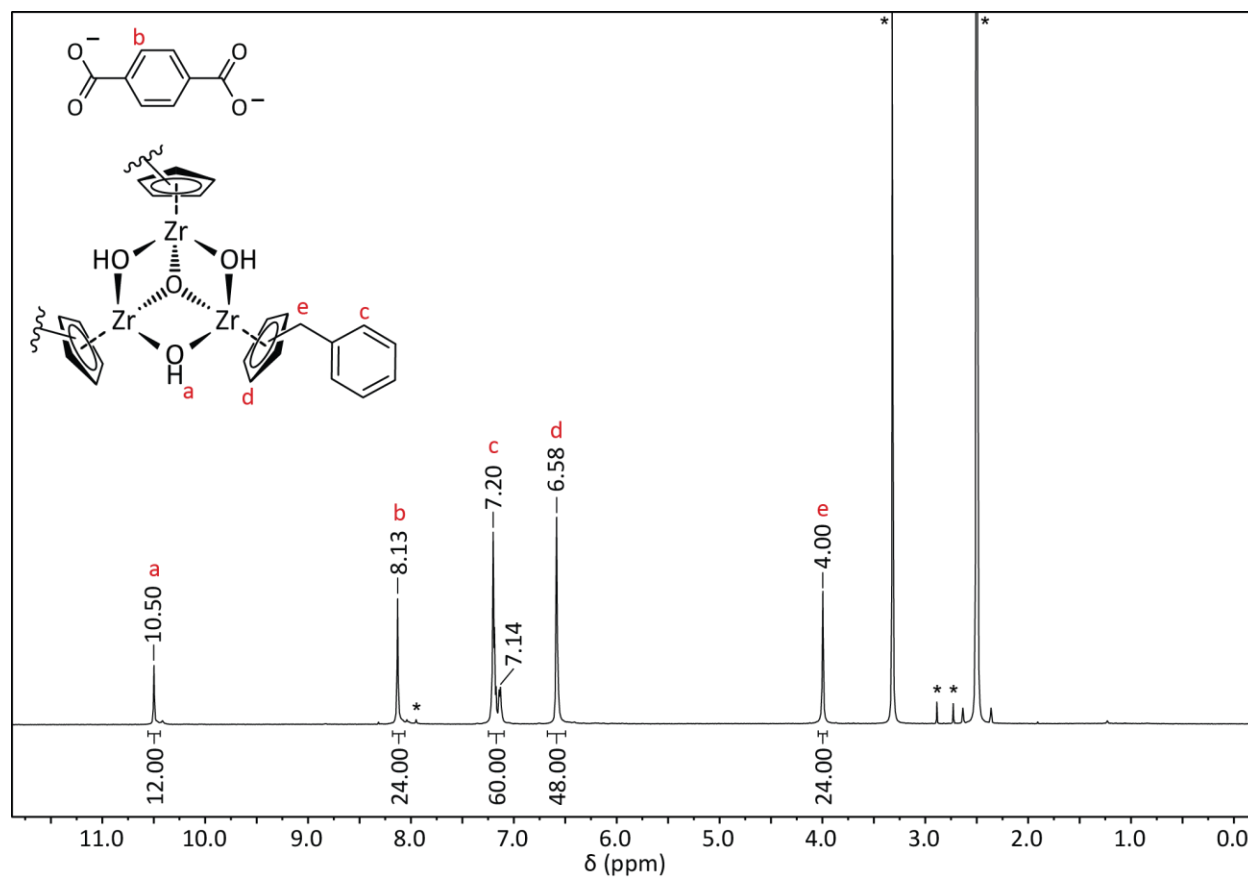


**Figure S12.**  $^1\text{H}$  NMR spectrum of ZrMOP-ben (500 MHz,  $\text{DMSO-d}_6$ ,  $25^\circ\text{C}$ ). Asterisks (\*) correspond to DMF (7.95, 2.89, 2.73 ppm),  $\text{H}_2\text{O}$  (3.34 ppm), and DMSO (2.50 ppm).

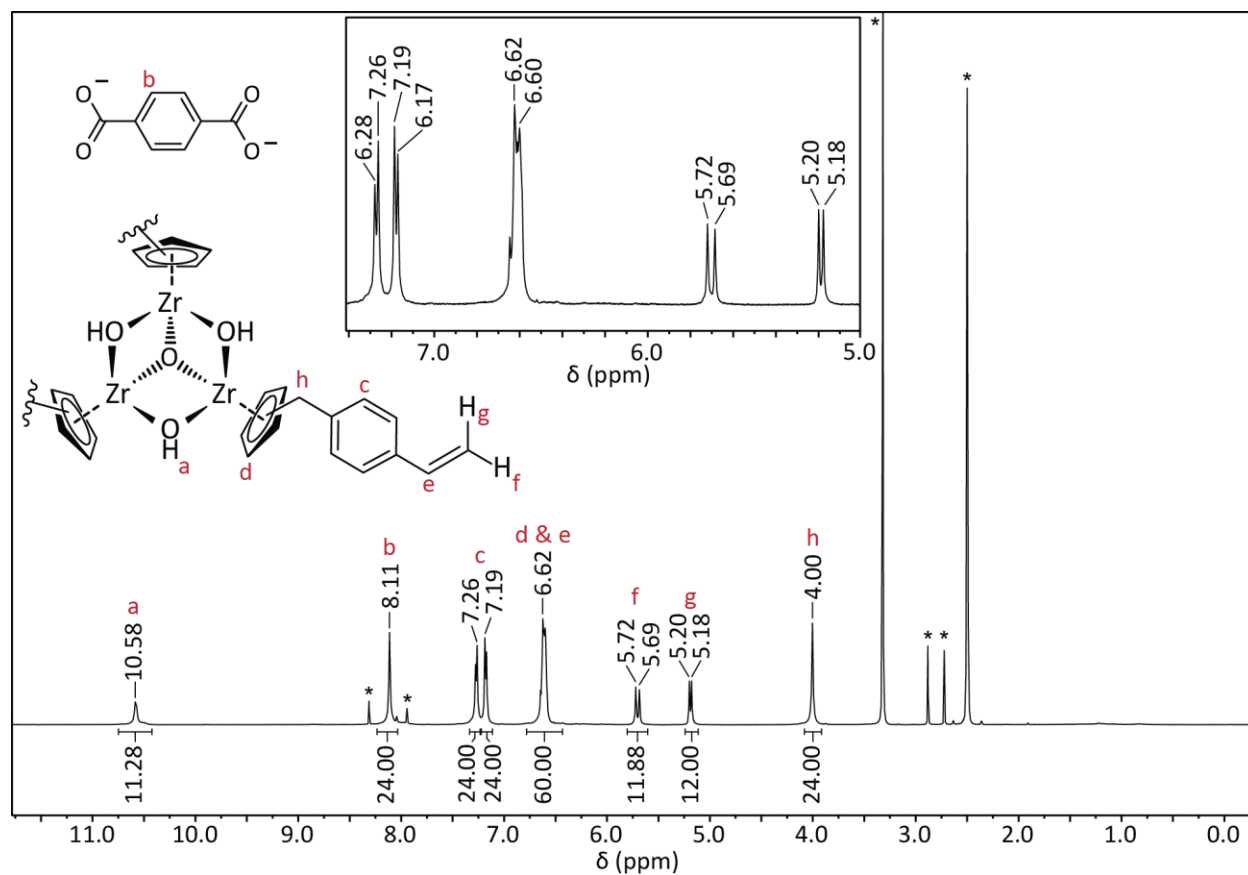


**Figure S13.**  $^1\text{H}$  NMR spectrum of  $\text{ZrMOP-vb}$  (500 MHz,  $\text{DMSO-d}_6$ ,  $25^\circ\text{C}$ ). Asterisks (\*) correspond to  $\text{CHCl}_3$  (8.31 ppm), DMF (7.95, 2.89, 2.73 ppm),  $\text{H}_2\text{O}$  (3.34 ppm), and DMSO (2.50 ppm).

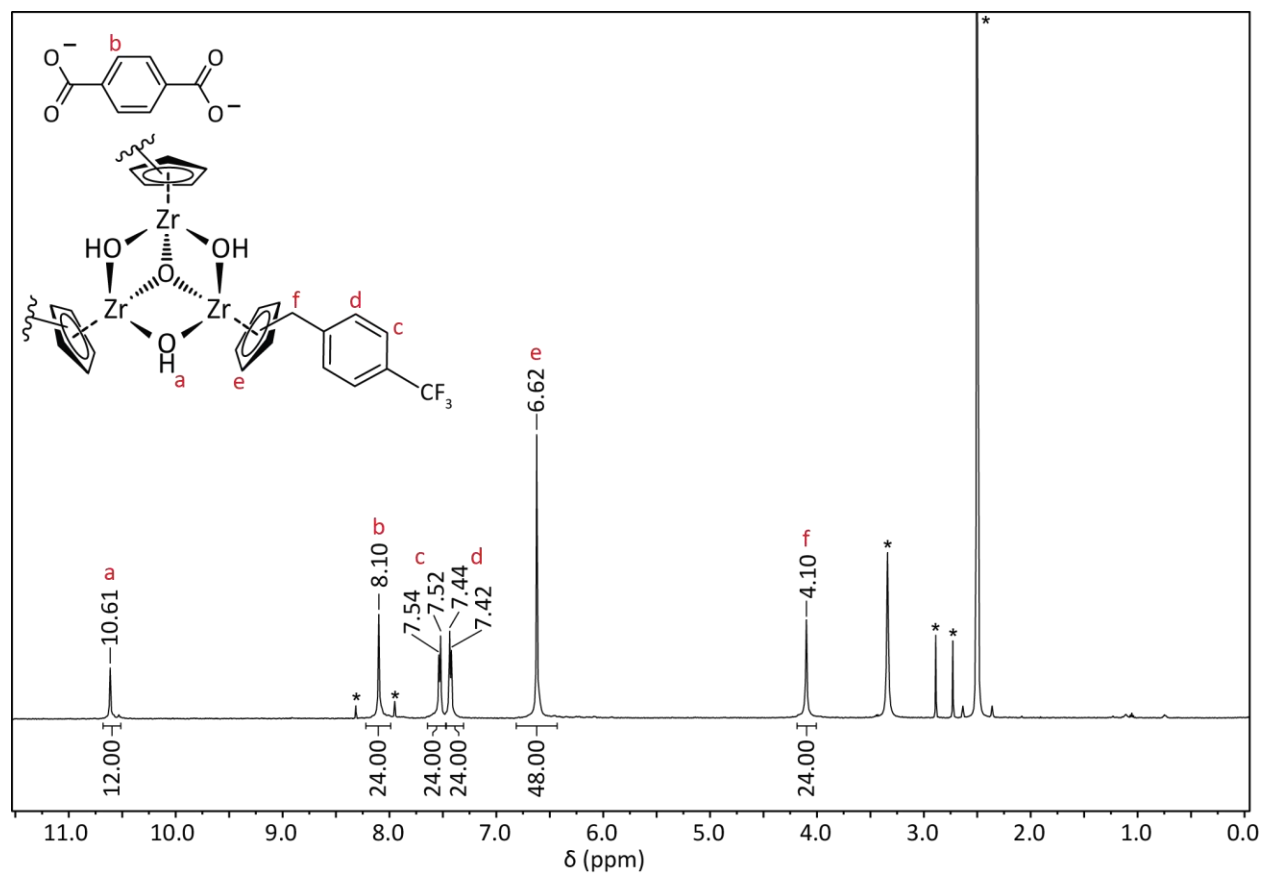


**Figure S14.** <sup>1</sup>H NMR spectrum of **ZrMOP-tfmb** (500 MHz, DMSO-d<sub>6</sub>, 25°C). Asterisks (\*) correspond to CHCl<sub>3</sub> (8.31 ppm), DMF (7.95, 2.89, 2.73 ppm), H<sub>2</sub>O (3.34 ppm), and DMSO (2.50 ppm).

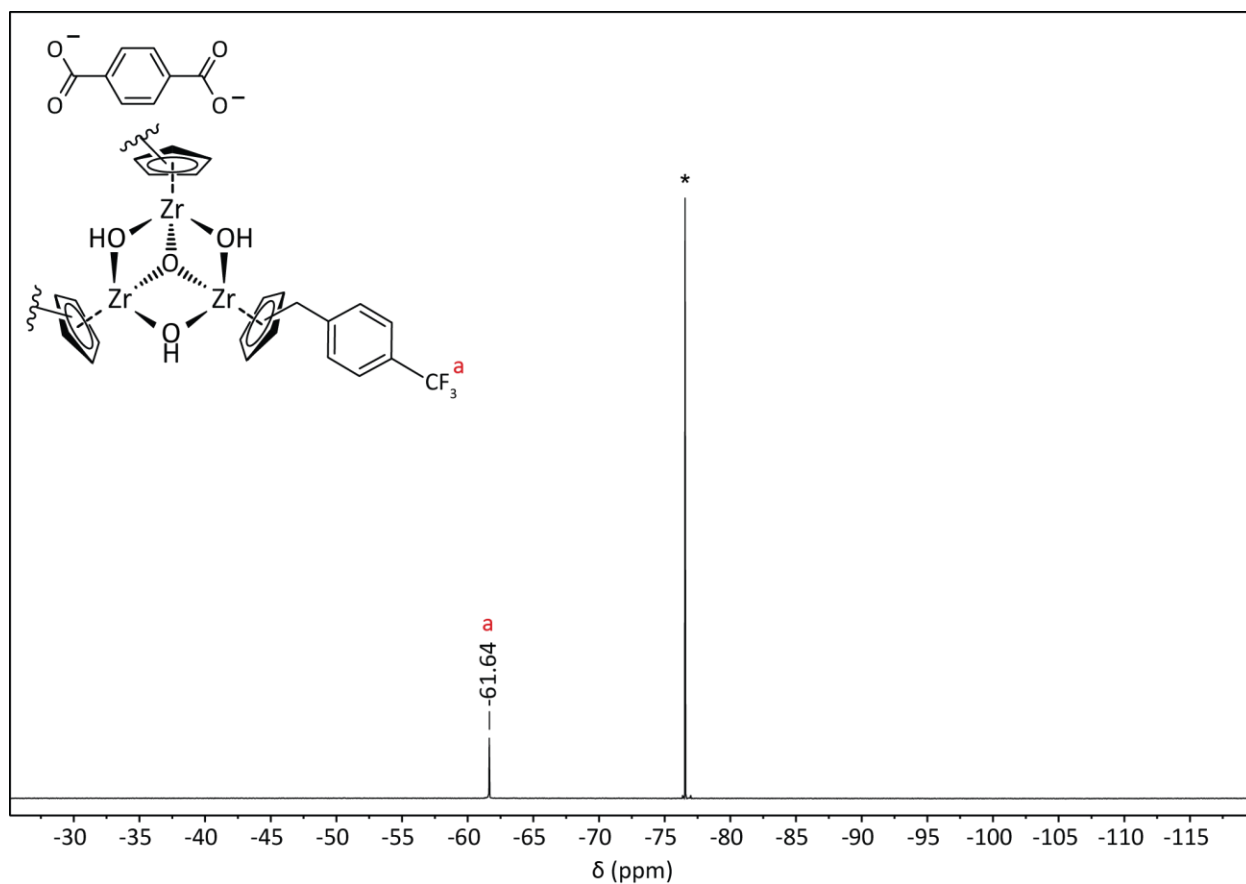


**Figure S15.**  $^{19}\text{F}$  NMR spectrum of **ZrMOP-tfmb** (470 MHz, DMSO- $d_6$ , 25°C). Asterisk (\*) corresponds to trifluoroacetic acid reference (-76.55 ppm).

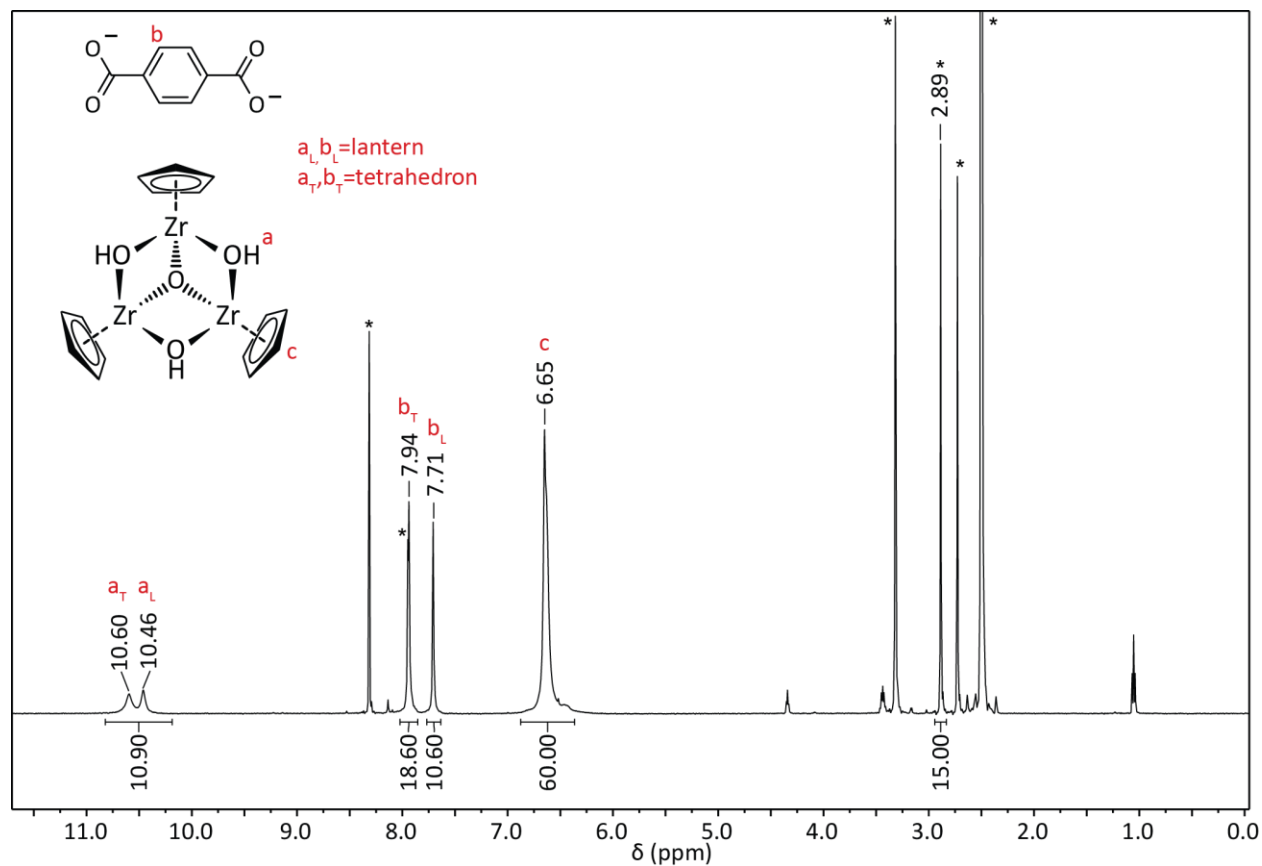


**Figure S16.** <sup>1</sup>H NMR spectrum of ZrMOP-bdc (500 MHz, DMSO-d<sub>6</sub>, 25°C) synthesized at 60°C for a longer reaction time. Asterisks (\*) correspond to CHCl<sub>3</sub> (8.31 ppm), DMF (7.95, 2.89, 2.73 ppm), H<sub>2</sub>O (3.34 ppm), and DMSO (2.50 ppm). μ-OH (10.60, 10.46 ppm) and 1,4-bdc (7.94, 7.71 ppm) peaks are labeled with their corresponding ZrMOP architecture (subscript “L” for V<sub>2</sub>L<sub>3</sub> lantern, subscript “T” for V<sub>4</sub>L<sub>6</sub> tetrahedron). CH<sub>3</sub> of DMF is integrated to show the contribution from the DMF CH (5H) under the 1,4-bdc CH signal at 7.94 ppm.

### Mass spectrometry

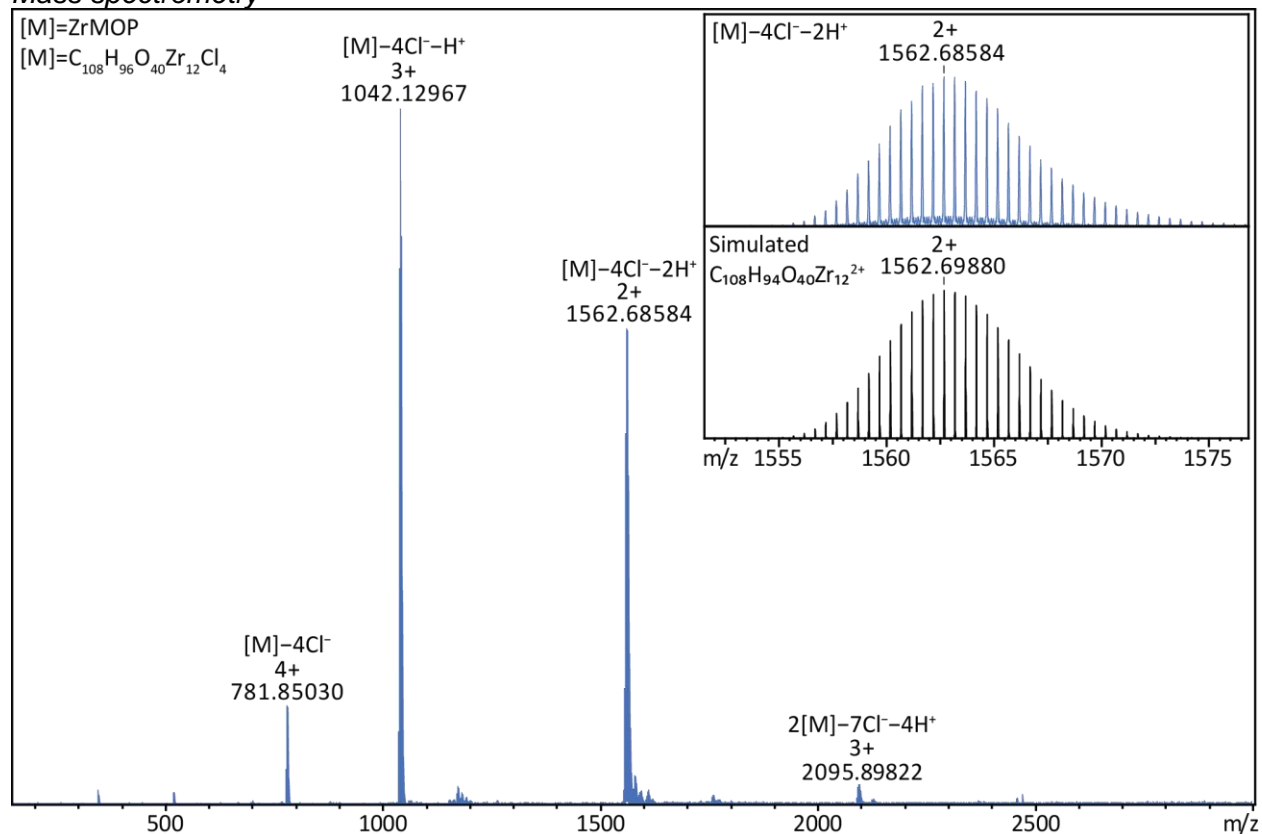


**Figure S17.** Full mass spectrum of **ZrMOP** in MeOH and the isotopic distribution of the 2+ cage with corresponding simulation.

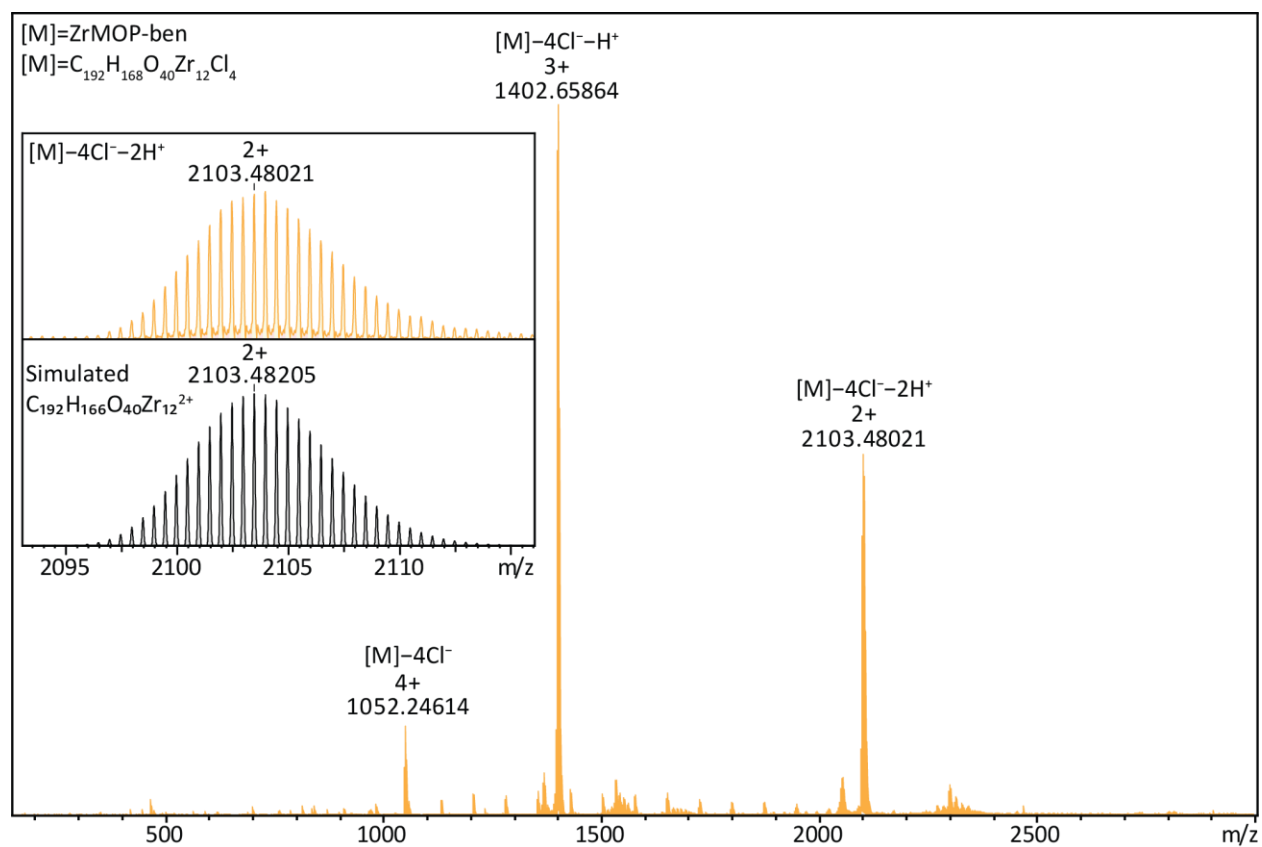


**Figure S18.** Full mass spectrum of **ZrMOP-ben** in MeOH and isotopic distribution of the 2+ cage with corresponding simulation.



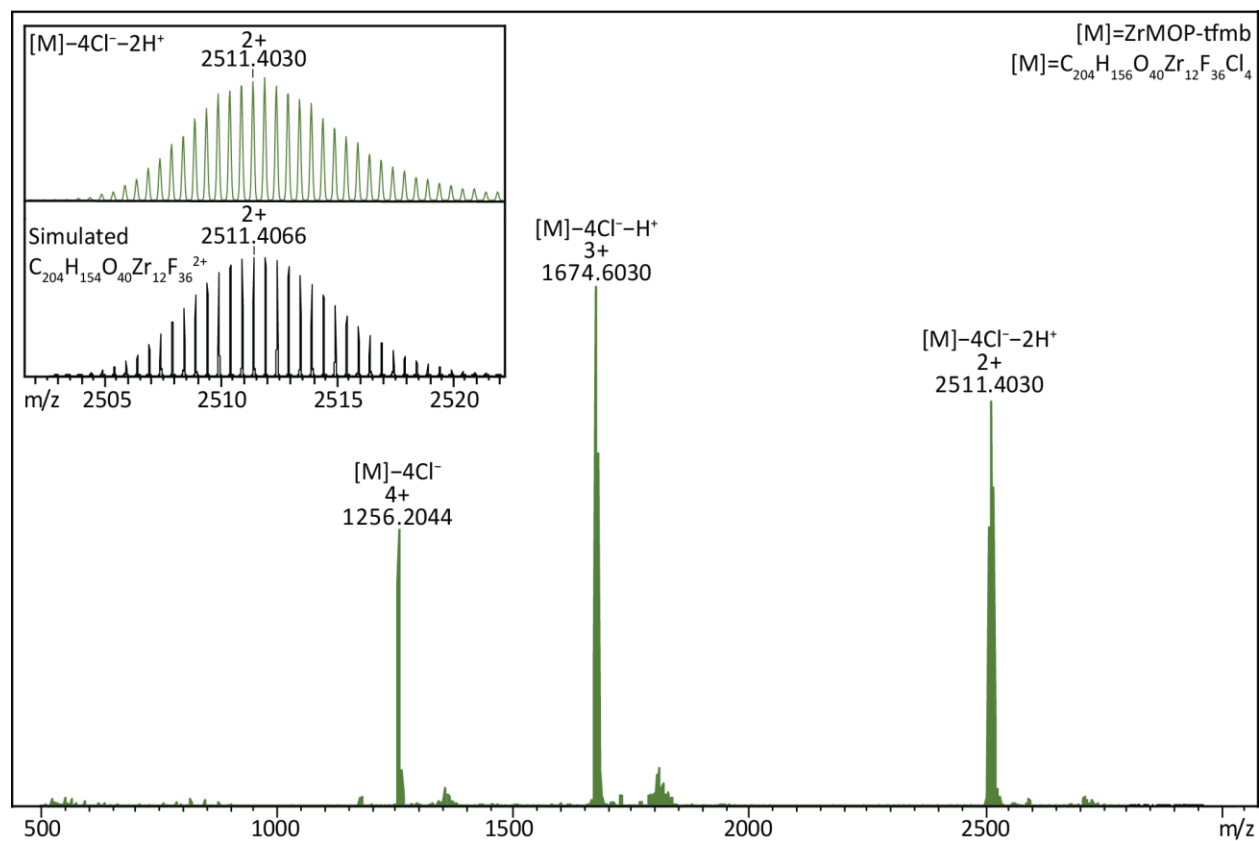


**Figure S20.** Full mass spectrum of ZrMOP-tfmb in MeOH and isotopic distribution of the 2+ cage with corresponding simulation.

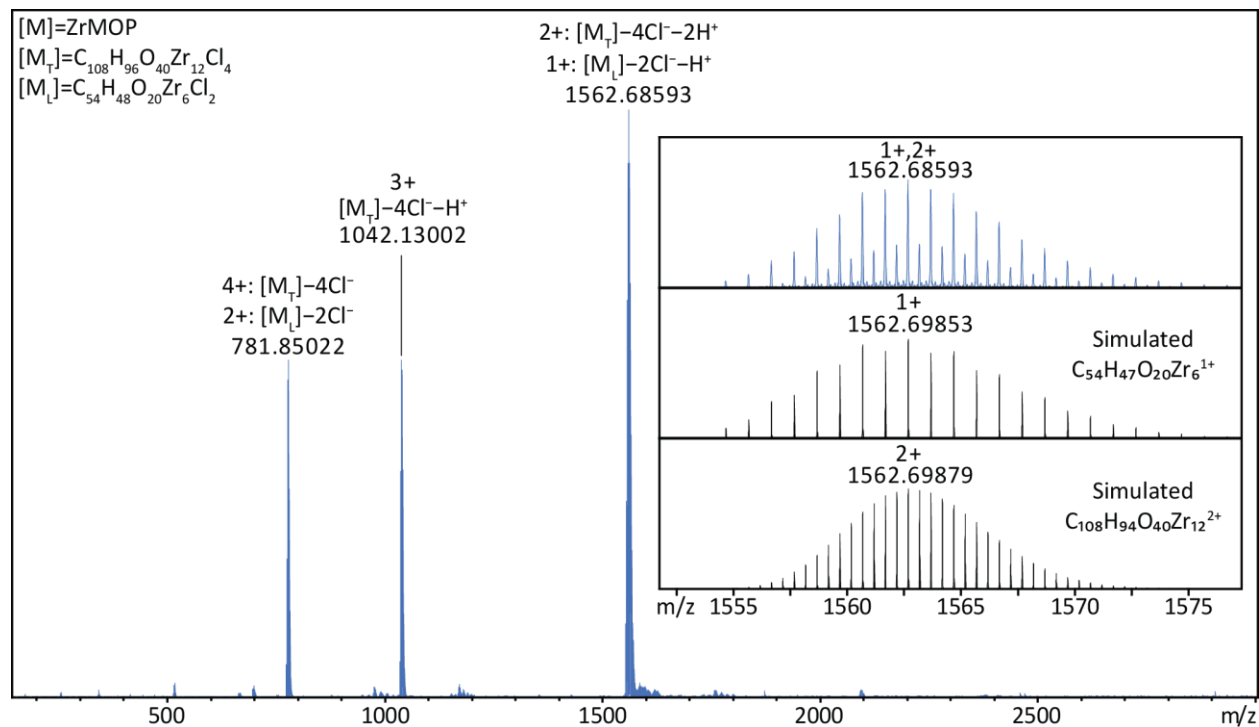


**Figure S21.** Full mass spectrum of ZrMOP-bdc, synthesized at 60°C for a longer reaction time, and characterized in MeOH.  $[M_T]$  corresponds to the tetrahedral ( $V_4L_6$ ) ZrMOP-bdc;  $[M_L]$  corresponds to the lantern ( $V_2L_3$ ) ZrMOP-bdc. Isotopic distribution of the 1+/2+ cages with corresponding simulations highlight the overlay of both patterns in the experimental pattern and thus presence of both architectures.

Infrared spectroscopy

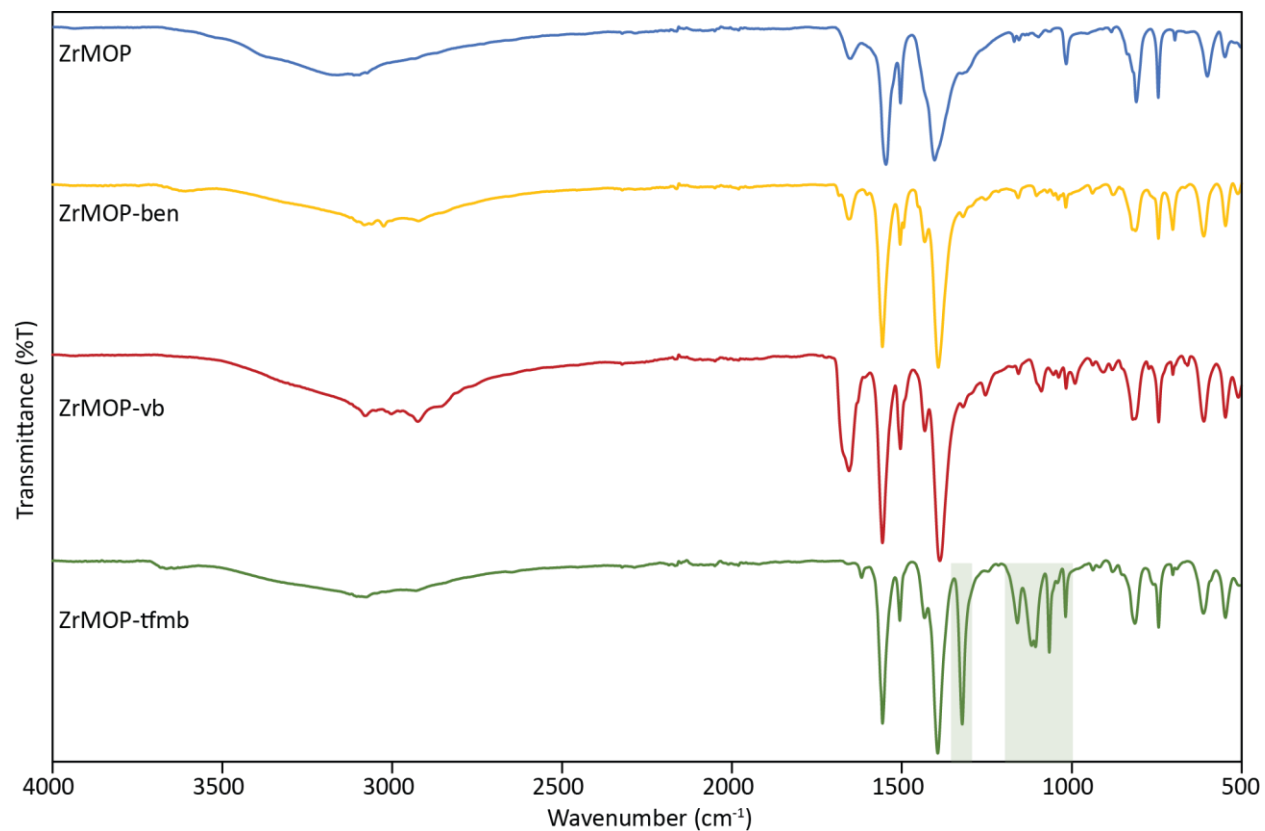


**Figure S22.** FTIR spectra of ZrMOPs showing CF<sub>3</sub> stretches at 1018 – 1161 cm<sup>-1</sup> and 1322 cm<sup>-1</sup>. Residual DMF appears at 1680 cm<sup>-1</sup>.

## X-Ray Crystallography

### Instrumental methods

Data sets for tetrahedra **ZrMOP-ben**, **ZrMOP-tfmb**, **ZrMOP-vb** and lanterns **ZrMOP-ben** and **ZrMOP-tfmb** were collected on a Rigaku XtaLAB synergy diffractometer equipped with a HyPix-6000HE detector and a PhotonJet Cu microfocus source. Crystals were cooled to 100 K during data collection using an Oxford 800 series cryostream. Crystals were suspended in paraffin oil and mounted on MiTeGen loops during data collection over the course of 24 hours. Structure solution was preformed using SHELXT with intrinsic phasing.<sup>1</sup> Structure refinement was carried out using SHELXL least-squares refinement within the Olex2 software package.<sup>2,3</sup> To expedite refinement CGLS was used initially, and structure were then finished with least squares cycles.

In general, the “core” (i.e. the Zr-clusters and 1,4-bdc ligands) of each tetrahedral, or lantern topology was easily found in the electron density map, and anisotropic refinement was performed. The pendant R-groups exhibited substantial positional disorder, in some cases (**ZrMOP-ben** lantern and tetrahedron, **ZrMOP-tfmb** lantern) the disorder was well-described by two position modeling. In the case of **ZrMOP-vb** and **ZrMOP-tfmb** tetrahedra the R-groups were heavily disordered over multiple positions. Several attempts were made to model these R-groups; however, the empirical electron density map proved too diffuse for chemically meaningful modeling, and therefore for these structures we have omitted the R-groups. In some cases, particularly when the Cp functionalities were interacting with adjacent tetrahedra, the R-groups were positionally locked due to intermolecular interactions. In these cases, the R-groups were well-behaved, and amenable to modeling. Ultimately, these two data sets are treated as “connectivity only”. The inability to completely model these vinyl benzyl and benzyl trifluoromethyl groups does not detract from the conclusions that a Zr-based MOP was synthesized and supports the topology formed. Hydrogen atoms were not located for connectivity-only structures.

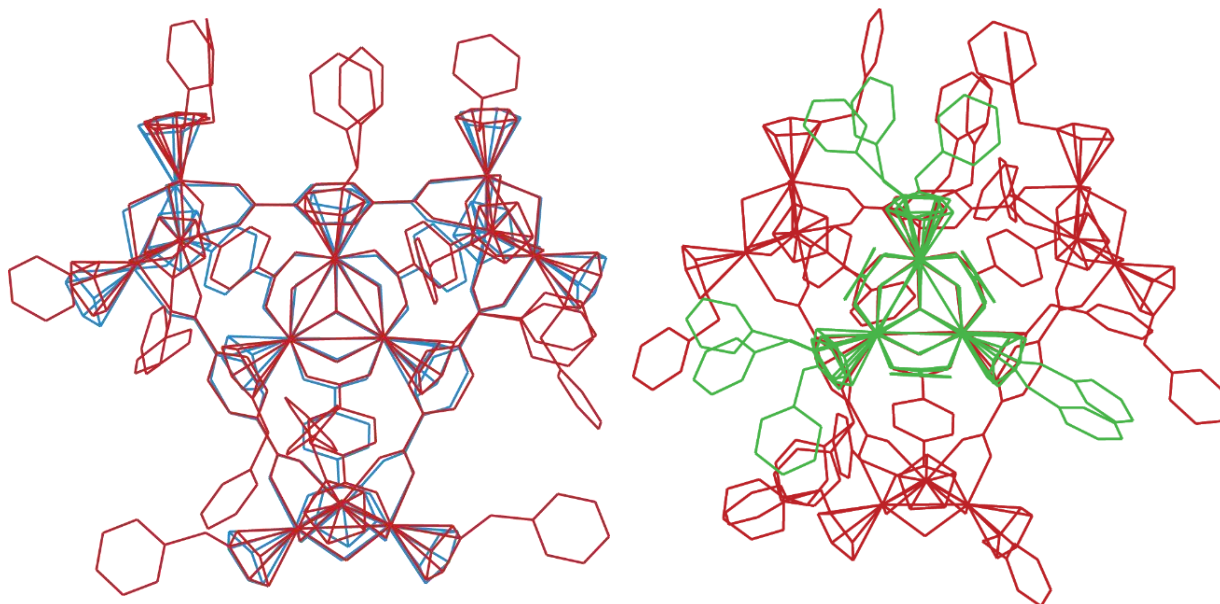


**Figure S23.** Overlay of **ZrMOP-ben** tetrahedron (red), unfunctionalized **ZrMOP** tetrahedron (blue)<sup>4</sup>, and **ZrMOP-ben** lantern (green).

## ZrMOP-ben

Table S1.

Crystallographic Details	ZrMOP-ben Lantern	ZrMOP-ben Tetrahedron
CCDC Number	2213860	2213859
Empirical formula	C <sub>102</sub> H <sub>98</sub> Cl <sub>2</sub> N <sub>2</sub> O <sub>22.5</sub> Zr <sub>6</sub>	C <sub>192</sub> H <sub>167</sub> Cl <sub>4</sub> O <sub>41</sub> Zr <sub>12</sub>
Formula weight	2330.04	4354.59
Temperature (K)	100.15	103.15
Crystal system	monoclinic	orthorhombic
Space group	<i>I</i> 2/ <i>a</i>	<i>Pbca</i>
<i>a</i> /Å	23.8868(3)	38.4705(2)
<i>b</i> /Å	14.9932(2)	42.4265(1)
<i>c</i> /Å	33.5014(3)	31.9924(1)
$\alpha$ /°	90	90
$\beta$ /°	103.661(1)	90
$\gamma$ /°	90	90
Volume/Å <sup>3</sup>	11658.7(2)	52217.0(3)
Z	4	8
$\rho_{\text{calc}}$ g/cm <sup>3</sup>	1.327	1.108
$\mu$ /mm <sup>-1</sup>	5.17	4.571
F(000)	4712	17464
Crystal size/mm <sup>3</sup>	0.12 × 0.097 × 0.048	0.242 × 0.184 × 0.103
Radiation	CuK $\alpha$ ( $\lambda$ = 1.54184)	CuK $\alpha$ ( $\lambda$ = 1.54184)
2 $\theta$ range for data collection/°	5.43 to 156.276	4.594 to 156.332
Index ranges	-27 ≤ <i>h</i> ≤ 30, -18 ≤ <i>k</i> ≤ 18, -42 ≤ <i>l</i> ≤ 42	-48 ≤ <i>h</i> ≤ 48, -51 ≤ <i>k</i> ≤ 53, -40 ≤ <i>l</i> ≤ 38
Reflections collected	65182	437426
Independent reflections	12303 [R <sub>int</sub> = 0.0376, R <sub>sigma</sub> = 0.0280]	55533 [R <sub>int</sub> = 0.0693, R <sub>sigma</sub> = 0.0336]
Data/restraints/parameters	12303/712/703	55533/743/2422
Goodness-of-fit on F <sup>2</sup>	1.054	1.064
Final R indexes [ <i>I</i> >= 2 $\sigma$ ( <i>I</i> )]	R <sub>1</sub> = 0.0678, wR <sub>2</sub> = 0.1992	R <sub>1</sub> = 0.0851, wR <sub>2</sub> = 0.1949
Final R indexes [all data]	R <sub>1</sub> = 0.0766, wR <sub>2</sub> = 0.2098	R <sub>1</sub> = 0.0933, wR <sub>2</sub> = 0.2010
Largest diff. peak/hole / e Å <sup>-3</sup>	1.94/-0.88	1.82/-1.41

The unweighted R-factor is  $R_1 = \sum(F_o - F_c) / \sum F_o$ ;  $I > 2 \sigma(I)$  and the weighted R-factor is  $wR_2 = \{\sum w(F_o^2 - F_c^2)^2 / \sum w(F_o^2)^2\}^{1/2}$

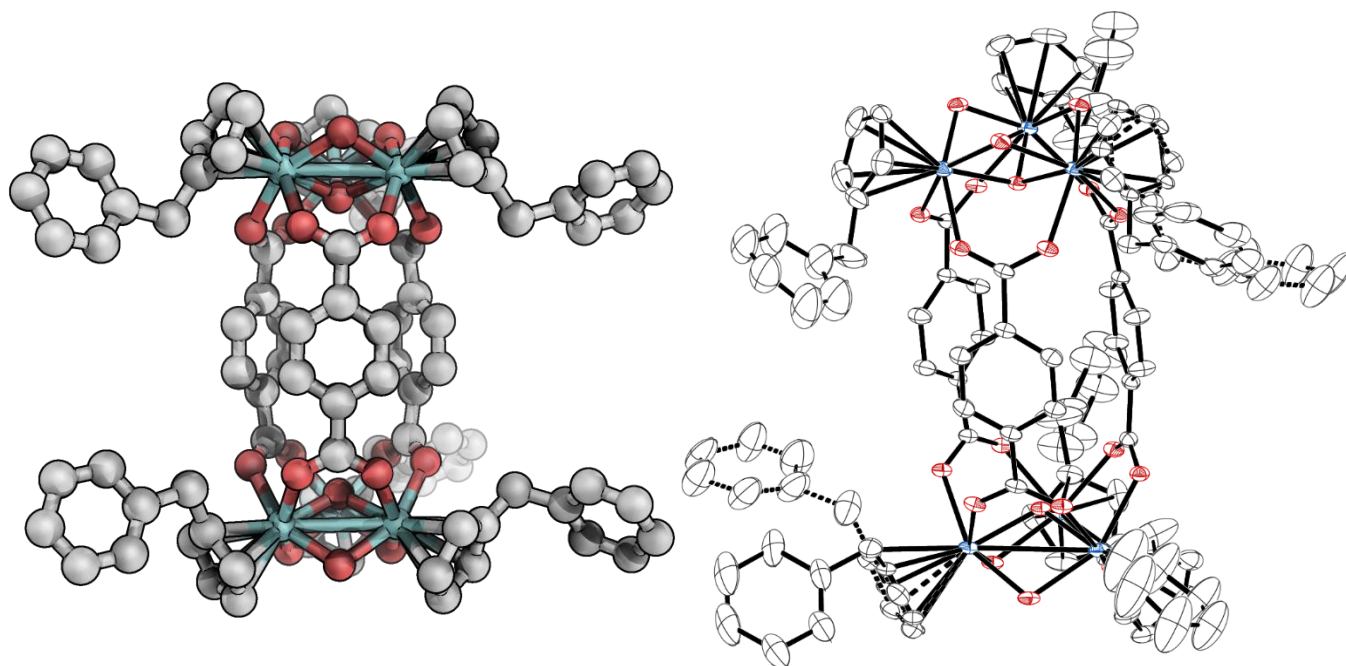


**Figure S24.** ZrMOP-ben lantern (left) with ORTEP (right) with thermal ellipsoids set to a 20% probability level. Hydrogens, counterions, and solvent omitted for clarity.

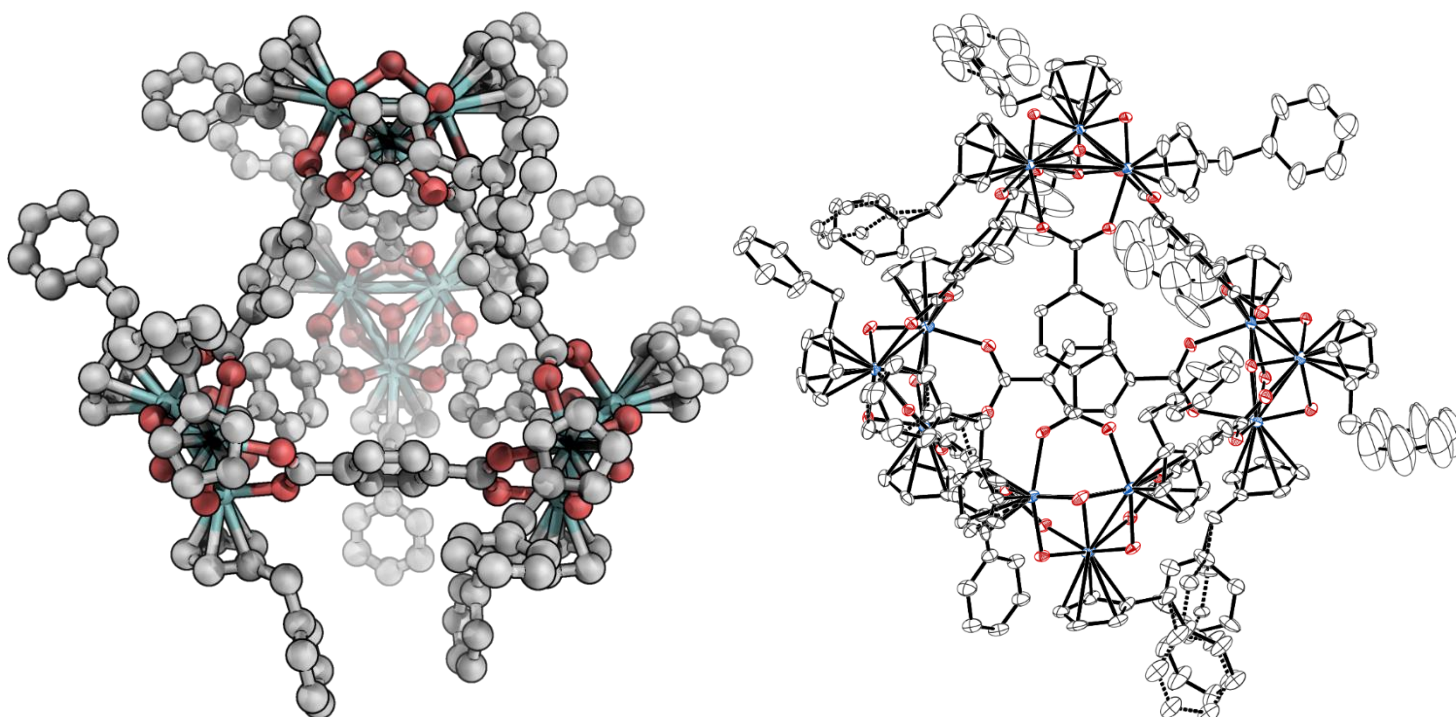


**Figure S25.** ZrMOP-ben tetrahedron (left) with ORTEP (right) with thermal ellipsoids set to a 20% probability level. Hydrogens, counterions, and solvent omitted for clarity.

ZrMOP-vb  
Table S2.

Crystallographic Details	ZrMOP-vb Tetrahedron
CCDC Number	2214055
Empirical formula	C <sub>139.83</sub> H <sub>118.67</sub> Cl <sub>4</sub> O <sub>41.33</sub> Zr <sub>12</sub> • 15.7DMF
Formula weight	3591.18
Temperature (K)	101.15
Crystal system	triclinic
Space group	<i>P</i> -1
<i>a</i> /Å	31.9619(3)
<i>b</i> /Å	35.5863(3)
<i>c</i> /Å	42.8112(4)
$\alpha$ /°	86.160(1)
$\beta$ /°	86.329(1)
$\gamma$ /°	63.715(1)
Volume/Å <sup>3</sup>	43528.7(8)
Z	6
$\rho$ calcg/cm <sup>3</sup>	0.822
$\mu$ /mm <sup>-1</sup>	4.050
F(000)	10348.0
Crystal size/mm <sup>3</sup>	0.403 × 0.26 × 0.225
Radiation	CuK $\alpha$ ( $\lambda$ = 1.54184)
2 $\theta$ range for data collection/°	4.14 to 133.9
Index ranges	-37 ≤ <i>h</i> ≤ 38, -41 ≤ <i>k</i> ≤ 42, -50 ≤ <i>l</i> ≤ 50
Reflections collected	701220
Independent reflections	150901 [R <sub>int</sub> = 0.0889, R <sub>sigma</sub> = 0.0531]
Data/restraints/parameters	150901/8818/4854
Goodness-of-fit on F <sup>2</sup>	1.275
Final R indexes [ <i>I</i> ≥ 2 $\sigma$ ( <i>I</i> )]	R <sub>1</sub> = 0.1233, wR <sub>2</sub> = 0.3593
Final R indexes [all data]	R <sub>1</sub> = 0.1620, wR <sub>2</sub> = 0.3956
Largest diff. peak/hole / e Å <sup>-3</sup>	1.63/-0.79

The unweighted R-factor is  $R_1 = \sum(F_o - F_c) / \sum F_o$ ;  $I > 2 \sigma(I)$  and the weighted R-factor is  $wR_2 = \{ \sum w(F_o^2 - F_c^2)^2 / \sum w(F_o^2)^2 \}^{1/2}$

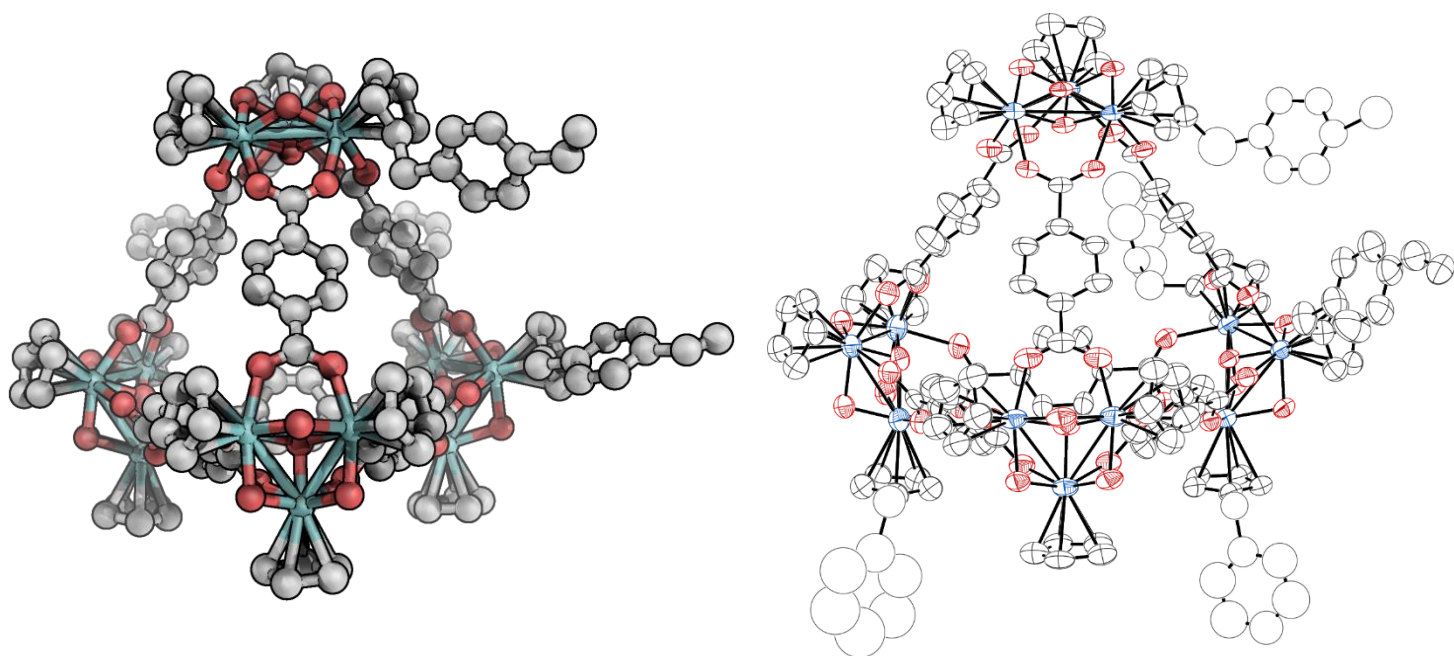


**Figure S26.** Connectivity structure of **ZrMOP-vb** tetrahedron (left) with ORTEP (right) with thermal ellipsoids set to a 20% probability level. Hydrogens, counterions, and solvent omitted for clarity. R-groups omitted were not modelable.

## ZrMOP-tfmb

Table S3.

Crystallographic Details	ZrMOP-tfmb Lantern	ZrMOP-tfmb Tetrahedron
CCDC Number	2213861	2214064
Empirical formula	C <sub>108</sub> H <sub>92</sub> Cl <sub>2</sub> F <sub>18</sub> N <sub>2</sub> O <sub>22</sub> Zr <sub>6</sub>	C <sub>155</sub> H <sub>123.5</sub> Cl <sub>4</sub> F <sub>15</sub> N <sub>0.5</sub> O <sub>40</sub> Zr <sub>12</sub> • 23DMF
Formula weight	2730.05	8324.95
Temperature (K)	101.15	101.15
Crystal system	triclinic	monoclinic
Space group	<i>P</i> -1	<i>C</i> 2/ <i>c</i>
<i>a</i> /Å	17.6615(2)	35.5390(7)
<i>b</i> /Å	22.1534(4)	32.1758(3)
<i>c</i> /Å	22.8454(4)	105.667(1)
$\alpha$ /°	67.304(2)	90
$\beta$ /°	69.669(1)	94.954(1)
$\gamma$ /°	83.237(1)	90
Volume/Å <sup>3</sup>	7731.3(2)	120378(3)
Z	2	8
$\rho$ calcg/cm <sup>3</sup>	1.173	0.919
$\mu$ /mm <sup>-1</sup>	4.14	4.020
F(000)	2732	33024.0
Crystal size/mm <sup>3</sup>	0.259 × 0.156 × 0.121	N/A
Radiation	CuK $\alpha$ ( $\lambda$ = 1.54184)	CuK $\alpha$ ( $\lambda$ = 1.54184)
2 $\theta$ range for data collection/°	4.324 to 156.954	4.16 to 103.668
Index ranges	-22 ≤ <i>h</i> ≤ 22, -26 ≤ <i>k</i> ≤ 28, -28 ≤ <i>l</i> ≤ 29	-23 ≤ <i>h</i> ≤ 21, -32 ≤ <i>k</i> ≤ 32, -107 ≤ <i>l</i> ≤ 107
Reflections collected	199421	129856
Independent reflections	32574 [R <sub>int</sub> = 0.0609, R <sub>sigma</sub> = 0.0407]	48746 [R <sub>int</sub> = 0.0587, R <sub>sigma</sub> = 0.0700]
Data/restraints/parameters	32574/1105/1601	48746/3880/3265
Goodness-of-fit on F <sup>2</sup>	1.097	1.057
Final R indexes [ <i>I</i> ≥ 2 $\sigma$ ( <i>I</i> )]	R <sub>1</sub> = 0.0743, wR <sub>2</sub> = 0.2406	R <sub>1</sub> = 0.1006, wR <sub>2</sub> = 0.2973
Final R indexes [all data]	R <sub>1</sub> = 0.0831, wR <sub>2</sub> = 0.2529	R <sub>1</sub> = 0.1231, wR <sub>2</sub> = 0.3179
Largest diff. peak/hole / e Å <sup>-3</sup>	1.15/-1.11	2.15/-0.64

The unweighted R-factor is  $R_1 = \sum(F_o - F_c)/\sum F_o$ ;  $I > 2 \sigma(I)$  and the weighted R-factor is  $wR_2 = \{\sum w(F_o^2 - F_c^2)^2 / \sum w(F_o^2)^2\}^{1/2}$

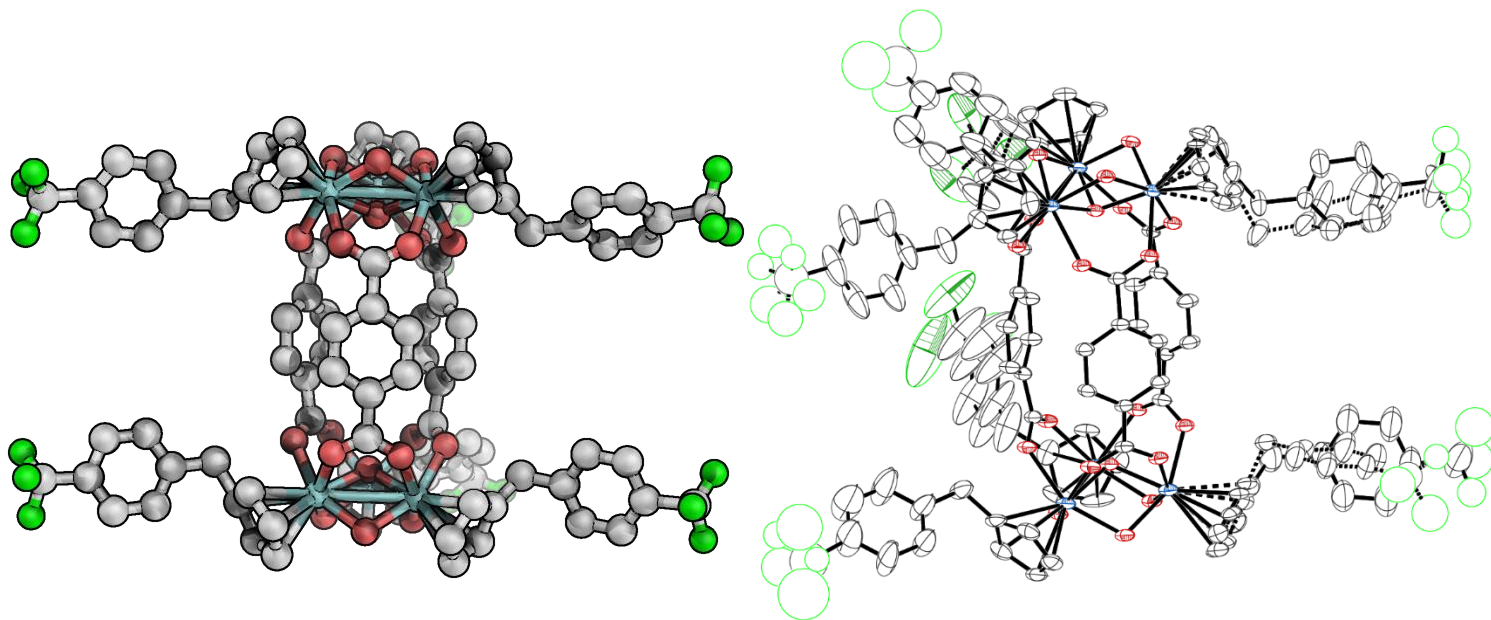


**Figure S27.** ZrMOP-tfmb lantern (left) with ORTEP (right) with thermal ellipsoids set to a 20% probability level. Hydrogens, counterions, and solvent omitted for clarity.

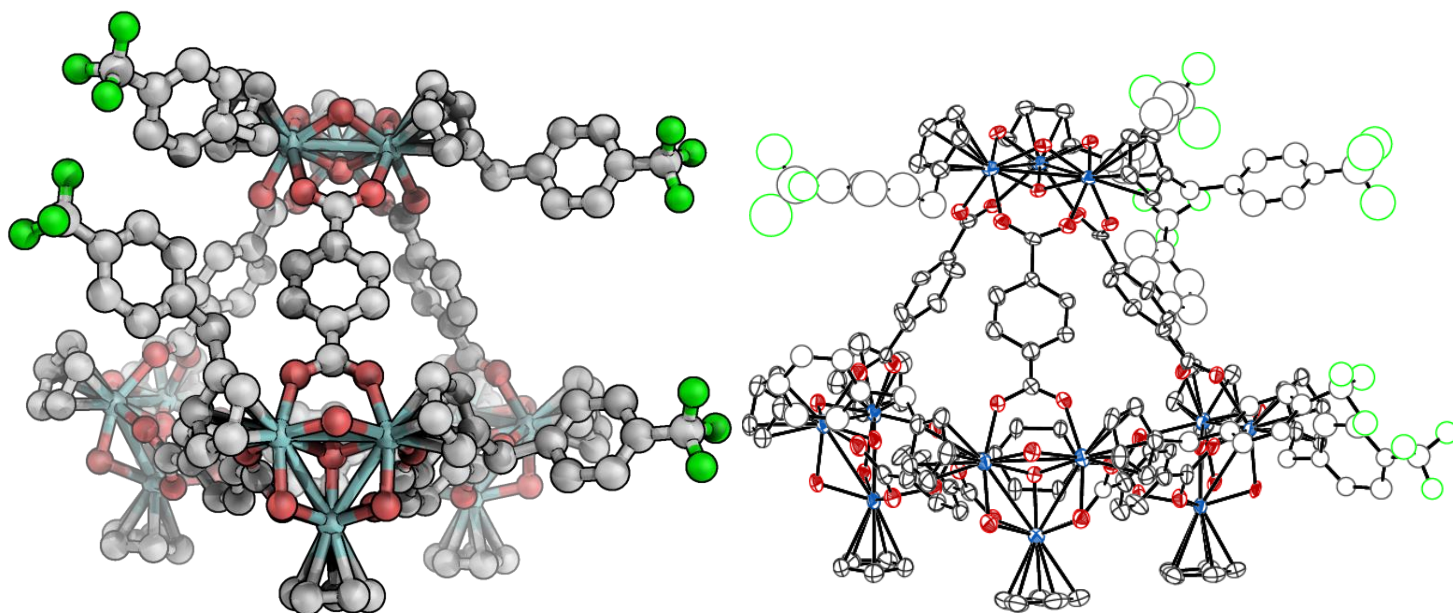


**Figure S28.** Connectivity structure of ZrMOP-tfmb tetrahedron (left) with ORTEP (right) with thermal ellipsoids set to a 20% probability level. Hydrogens, counterions, and solvent omitted for clarity. R-groups omitted were not model-able.

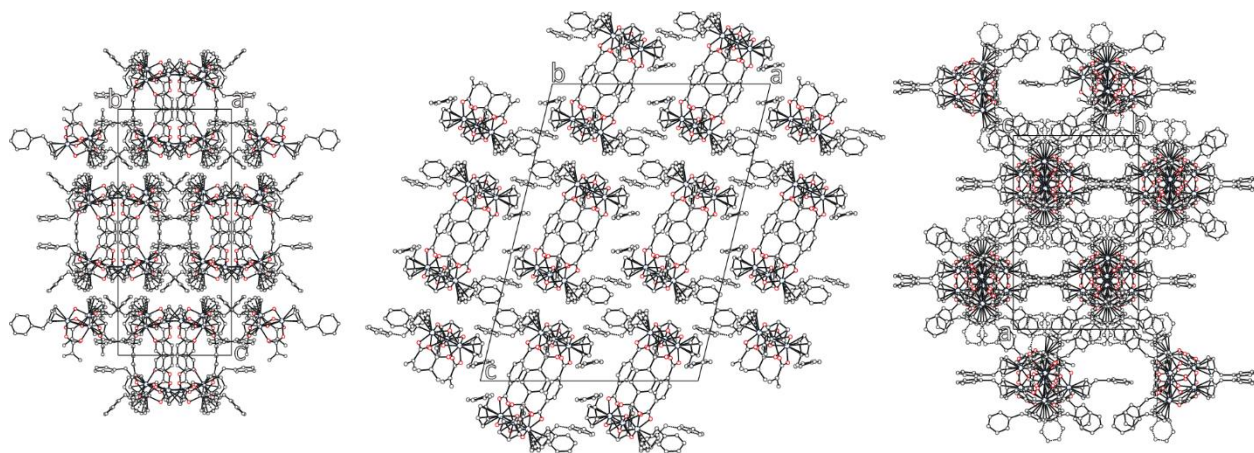


**Figure S29.** ZrMOP-ben lantern unit cell packed with complete molecular fragments viewed along the crystallographic *a*, *b*, and *c* directions (left to right). Counterions, hydrogen atoms, and solvents omitted for clarity.

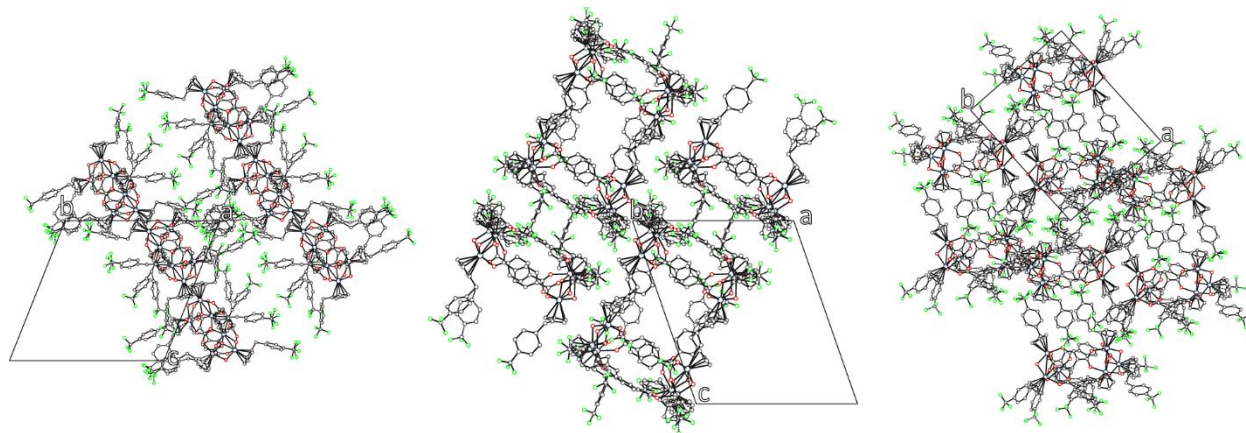


**Figure S30.** ZrMOP-tfmb lantern unit cell packed to limits  $\pm 0.5$  along *a*, *b*, *c* viewed along the crystallographic *a*, *b*, and *c* directions (left to right). Counterions, hydrogen atoms, and solvents omitted for clarity.

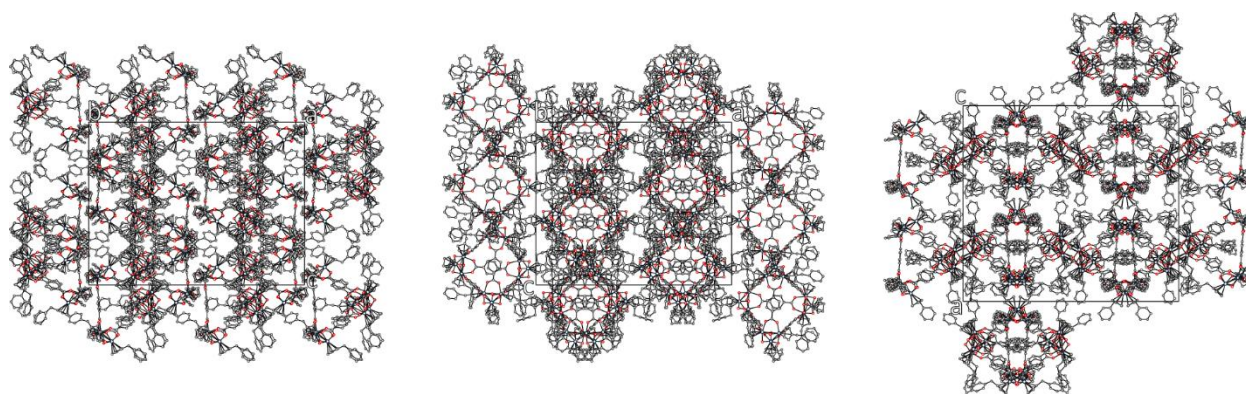


**Figure S31.** ZrMOP-ben tetrahedron unit cell packed with complete molecular fragments viewed along the crystallographic *a*, *b*, and *c* directions (left to right). Counterions, hydrogen atoms, and solvents omitted for clarity.

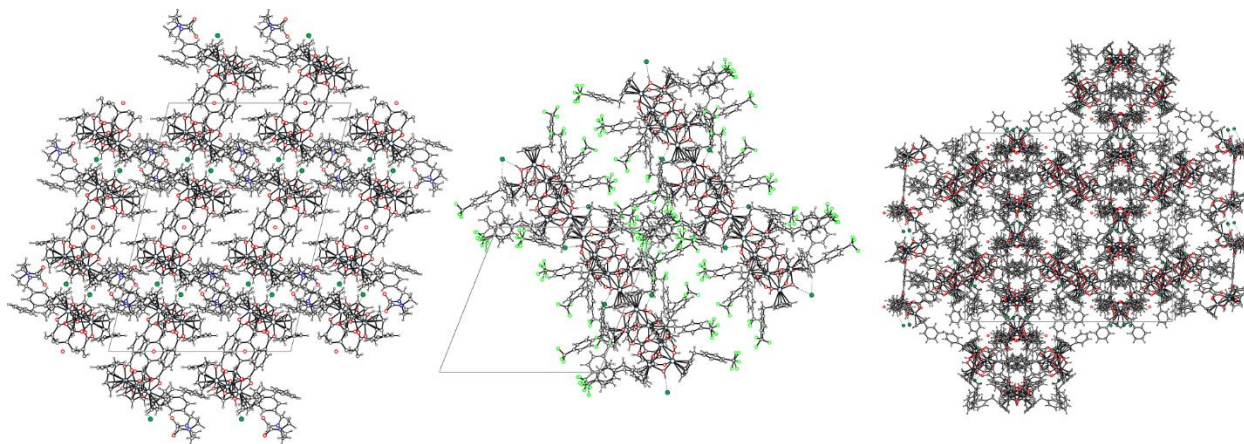


**Figure S32.** ZrMOP-ben lantern, ZrMOP-tfmb lantern, and ZrMOP-ben tetrahedron (left to right) packed with complete molecular fragments with counterions and modeled solvent molecules showing distinct hydrogen bond networks in the crystal packing.

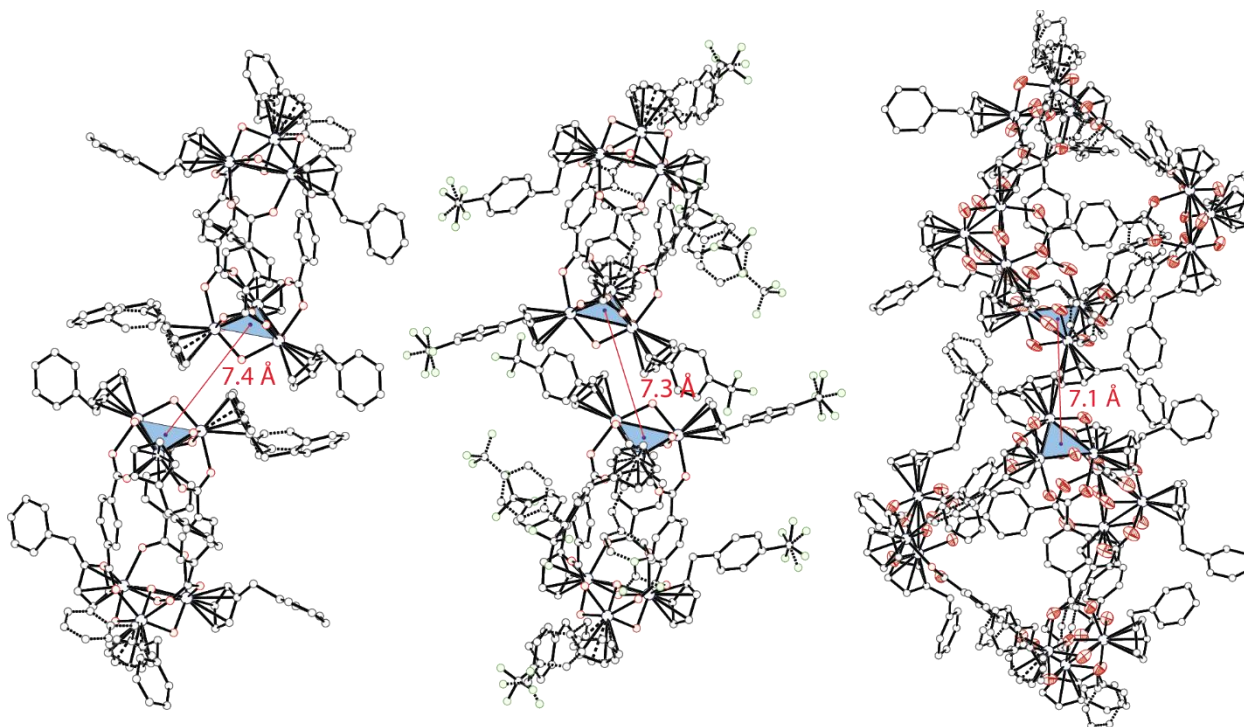


**Figure S33.** ZrMOP-ben lantern, ZrMOP-tfmb lantern, and ZrMOP-ben tetrahedron (left to right) with Zr-Zr-Zr plane and centroid shown on structure, with separation distances. Counterions, hydrogen atoms, and solvents omitted for clarity.

## Solubility Studies

### *Instrumental methods*

ThermoElectron X Series 2 ICP-MS was used for quantitative analysis of zirconium content. Collision cell technology (CCT) was used with helium to minimize polyatomic interferences. Three injections were run per sample, with minimal variance apparent (<2% relative standard deviation).

### *Materials*

Zirconium standard solution (1000 mg/L ZrCl<sub>4</sub> in 2 M HCl) was purchased from Sigma Aldrich. Cobalt standard solution (10.00 µg/mL in 3% v/v HNO<sub>3</sub>) was purchased from Inorganic Ventures. Metal-free nitric acid (67-70% w/w) was purchased from VWR Chemicals. Nanopure water was obtained from a Thermo Scientific Barnstead Nanopure water purification system, and was used for all dilutions, as well as samples prepared in water. Methanol and dimethyl sulfoxide were purchased from Fisher Chemical, and dimethylformamide was purchased from Sigma Aldrich.

### *Solution preparation & digestion*

Three independent batches were synthesized of each **ZrMOP**, **ZrMOP-ben**, **ZrMOP-vb**, and **ZrMOP-tfmb**. Each batch of each ZrMOP was added in excess to four 1-dram vials with a stir bars. About 2 mL of each solvent (water, methanol, DMF, DMSO) was added to one sample per batch across three batches, totaling twelve samples made per ZrMOP, with each solvent represented in triplicate. The suspensions were stirred at room temperature for 1 hour. This was done side-by-side with water, methanol, DMF, and DMSO solvent blanks stirring in 1-dram vials, totaling 52 samples prepared.

After 1 hour, the stir bars were removed from the suspensions, and each suspension was carefully filtered through 1-1.5 inches of packed celite atop a microfiber filter paper in a glass pipette. This was assisted by vacuum filtration. The resulting clear solutions were filtered into clean 1-dram vials. 100 µL of each saturated solution was then added by micropipette to a clean 2-dram vial containing 1 mL of metal free nitric acid. The vials were loosely capped and were allowed to off-gas at room temperature overnight. The next morning, all 52 samples were placed in a 40°C oil bath. Temperature was increased in 5°C increments to 60°C over the course of a few hours, being sure that vials were properly vented if off-gassing was still occurring. The samples were left to digest at 60°C for three days, after which they were no longer off-gassing, and were allowed to cool to room temperature.

Each of the 52 samples was diluted to 25 mL (100 µL to 25 mL) with water in a volumetric flask. Samples in water, as well as **ZrMOP** in DMF, were not diluted any further. All samples prepared in methanol and DMSO were diluted again (1 mL to 25 mL), as well as the benzyl-, vinylbenzyl-, and trifluoromethyl-functionalized ZrMOPs in DMF (1 mL to 25 mL), with 2.5% nitric acid solution. Solvent blanks were diluted in an analogous fashion. As an internal standard, 125 µL of cobalt standard solution was added to each sample to a final concentration of 50 ppb. This was used to correct for instrument drift and matrix effects.

### *Instrument Calibration*

Standard solutions of zirconium were prepared through independent dilutions of 1000 ppm zirconium standard to final concentrations of 10, 25, 50, 75, 100, 200, 300, and 400 ppb. These samples were used to construct the following Zr-90 and Zr-91 calibration curve (Figures S34, S35). The Zr-91 calibration curve ( $R^2=0.9999$ ) was used to determine unknown concentrations of zirconium in ZrMOP samples.

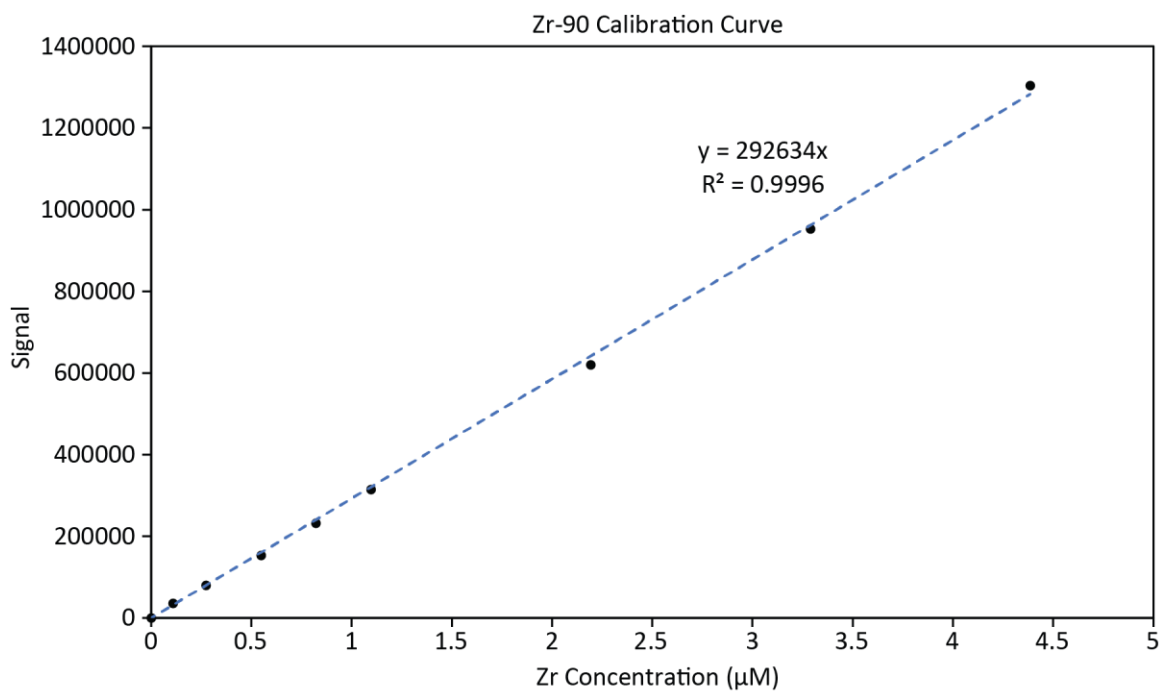


**Figure S34.** Zirconium-90 ICP-MS calibration data with linear trendline and fit.

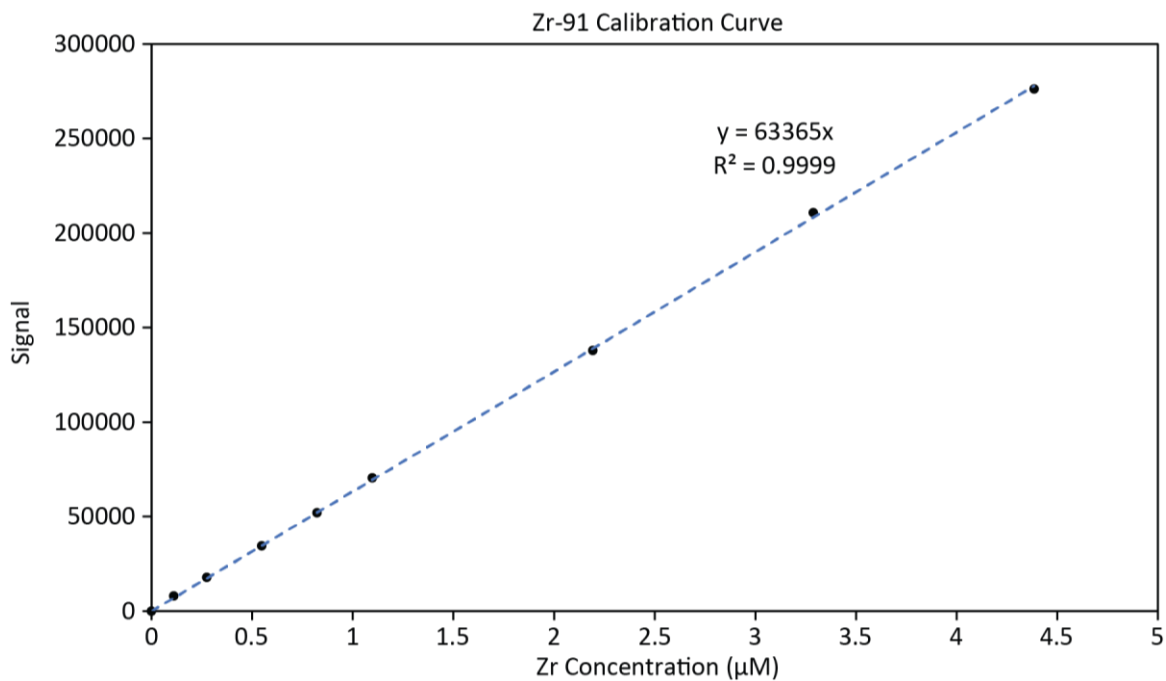


**Figure S35.** Zirconium-91 ICP-MS calibration data with linear trendline and fit.

## Results

**Table S4.** Results of ICP-MS solubility studies for ZrMOPs in water.

ZrMOP Concentration ( $\mu\text{M}$ ) in Water					
MOP	Batch 1	Batch 2	Batch 3	Average	Relative Standard Deviation (%)
ZMOP	11.8	10.3	9.80	10.6	9.6
ZrMOP-ben	1.49	1.71	1.82	1.67	10.3
ZrMOP-vb	1.27	1.83	1.72	1.60	18.5
ZrMOP-tfmb	1.43	1.39	1.25	1.36	6.7

**Table S5.** Results of ICP-MS solubility studies for ZrMOPs in methanol.

ZrMOP Concentration (mM) in Methanol					
MOP	Batch 1	Batch 2	Batch 3	Average	Relative Standard Deviation (%)
ZMOP	2.35	1.69	1.92	1.98	17.0
ZrMOP-ben	0.48	0.56	0.53	0.52	7.5
ZrMOP-vb	1.38	0.72	0.52	0.87	51.3
ZrMOP-tfmb	0.51	0.50	0.66	0.55	16.0

**Table S6.** Results of ICP-MS solubility studies for ZrMOPs in DMSO.

ZrMOP Concentration (mM) in DMSO					
MOP	Batch 1	Batch 2	Batch 3	Average	Relative Standard Deviation (%)
ZMOP	1.15	0.87	1.01	1.01	14.2
ZrMOP-ben	0.75	1.18	1.10	1.01	22.4
ZrMOP-vb	1.74	1.47	1.36	1.52	12.8
ZrMOP-tfmb	0.71	0.77	0.79	0.76	5.4

**Table S7.** Results of ICP-MS solubility studies for ZrMOPs in DMF.

ZrMOP Concentration ( $\mu\text{M}$ ) in DMF					
MOP	Batch 1	Batch 2	Batch 3	Average	Relative Standard Deviation (%)
ZMOP	10.7	18.9	17.0	15.6	27.6
ZrMOP-ben	184	168	174	175	4.5
ZrMOP-vb	340	302	286	309	9.0
ZrMOP-tfmb	281	205	446	311	39.7

## References

1. G. Sheldrick, *Acta Crystallographica Section A*, 2015, **71**, 3-8.
2. G. Sheldrick, *Acta Crystallographica Section C*, 2015, **71**, 3-8.
3. O. V. Dolomanov, L. J. Bourhis, R. J. Gildea, J. A. K. Howard and H. Puschmann, *J. Appl. Crystallogr.*, 2009, **42**, 339-341.
4. G. Liu, Z. Ju, D. Yuan and M. Hong, *Inorg. Chem.*, 2013, **52**, 13815-13817.